Neocortical differentiation and hippocampal integration of non-meaningful items and their spatial location

Zsuzsanna Nemecz[1,2,3], István Homolya[3,4], Alex Ilyés[1,2,3], Hunor Kis[1,2,3], György Mező[5,6], Virág Anna Varga[2,3], Markus Werkle-Bergner[7], Attila Keresztes[3,2]

1 Doctoral School of Psychology, ELTE Eötvös Loránd University, Budapest, Hungary
2 Institute of Psychology, ELTE Eötvös Loránd University, Budapest, Hungary
3 Brain Imaging Centre, HUN-REN Research Centre for Natural Sciences, Budapest
4 Budapest University of Technology and Economics, Budapest, Hungary
5 Wigner Datacenter, HUN-REN Wigner Research Centre for Physics, Budapest, Hungary
6 Konkoly Observatory, HUN-REN Research Centre for Astronomy and Earth Sciences, Budapest, Hungary
7 Center for Lifespan Psychology, Max Planck Institute for Human Development, Berlin Germany

Correspondence to: nemecz.zsuzsanna@ttk.hu, keresztes.attila.akk@ttk.hu

Abstract

Resolving interference between similar inputs is a critical feature of adaptive memory systems. Computational theories of the medial temporal lobe posit that the dentate gyrus and CA3 (CA3DG) subfields of the hippocampus are ideally suited to reduce interference via a process called pattern separation. Whereas neocortical areas upstream of the hippocampus have been shown to play a role in content-specific (e.g., spatial or object-related) interference reduction, the CA3DG is traditionally viewed as a domain-general pattern separator. Recent work also drew attention to the role of frontal and parietal control areas in allocating resources according to task demands during mnemonic discrimination, exerting top-down control over the medial temporal lobe. However, extant evidence in humans is almost solely based on mnemonic discrimination tasks involving everyday items, potentially confounding retrieval processes with pattern separation. Here, we studied pattern separation in a "process-pure" manner, utilizing non-meaningful fractal images. We acquired full-brain high-resolution functional MRI data of 39 participants (mean age (SD) = 22.6 (2.4) years, 19 females) while they studied fractals with varying degrees of interference in either their spatial or object features. Building upon the idea that the repetition of a stimulus results in a diminished BOLD response in areas involved in the processing of that stimulus (repetition suppression), we expected that regions engaged in pattern separation of objects or locations would decrease their response to repetitions, but not to highly similar (interference-inducing) items. We found that the parahippocampal cortex contributes to interference reduction in the spatial domain, while the perirhinal cortex contributes to interference reduction in the object domain. The frontoparietal control network was recruited during the encoding of both object and location lures, and displayed strengthened within- and cross-network connectivity in response to lures. Contrary to our expectations, the CA3DG showed repetition suppression to both exact repetitions and highly similar lures, indicating a lack of sensitivity to small differences in interfering stimuli. Altogether, these results are in line with content-specific neocortical interference reduction in the medial temporal lobe, possibly orchestrated by the frontoparietal control network, but challenge the view of CA3DG as a universal pattern separator.

Keywords: pattern separation, hippocampal subfields, interference resolution, fronto-parietal network

Introduction

Storing unique episodes in the face of interference from similar experiences is a challenge for adaptive memory systems (Kumaran et al., 2016; McCloskey & Cohen, 1989). Computational models of memory posit a process that encodes overlapping inputs in an independent manner, foregoing the danger of overwriting existing representations (McClelland et al., 1995; R. C. O'Reilly et al., 2014; O'Reilly & McClelland, 1994). This process of interference reduction is termed pattern separation (Marr, 1971; R. C. O'Reilly et al., 2014).

Decades of animal and human research have implicated the dentate gyrus and CA3 subfields of the hippocampus as the primary mnemonic pattern separator of the mammalian brain (Amer & Davachi, 2023; Leal & Yassa, 2018; Leutgeb et al., 2007; Rolls, 2013; Yassa & Stark, 2011). Neuroanatomical accounts propose that divergent excitatory projections from the entorhinal cortex to a large number of sparsely firing neurons expand the available representational space in the dentate gyrus (Cayco-Gajic & Silver, 2019). Consistent with this idea, rodent research has shown that even small changes in the environment induce decorrelated activity patterns in the dentate gyrus (GoodSmith et al., 2019; Knierim & Neunuebel, 2016; Leutgeb et al., 2007; Neunuebel & Knierim, 2014). Moreover, selectively disrupting dentate gyrus function in rats via lesions (Gilbert et al., 2001; Hunsaker et al., 2008) or the genetic knockout of the NR1 subunit of the NMDA receptor (McHugh et al., 2007) leads to impaired performance on tasks assumed to require spatial pattern separation. The dentate gyrus also appears to be necessary for odor discrimination in rats, especially at long delays, when the discrimination task has higher memory demands (Weeden et al., 2014). A recent study showed that serially presented images can be classified as new, repeated, or similar, based on single neuron recordings from the CA3 - dentate gyrus (CA3DG) of macaques, suggesting a highly distinct signal in this area in the primate brain (Sakon & Suzuki, 2019).

In humans, a rapidly growing number of behavioral, neuroimaging, and clinical studies investigates memory interference resolution. Behaviorally, mnemonic discrimination tasks, which require distinguishing previously encountered stimuli from similar lures, are thought to rely on hippocampal pattern separation. The most widely used of these is the Mnemonic Similarity Task (Stark et al., 2013, 2019), in which participants make old/similar/new recognition memory decisions about previously

viewed images of everyday objects. A flavor of this task was used to provide the first human neuroimaging evidence that the hippocampus processes lure stimuli differently from repeats (Kirwan & Stark, 2007). This study was soon followed by results specific to the CA3DG, which showed that levels of lure-related activity were comparable to new trials (Bakker et al., 2008). Functional magnetic resonance (fMRI) imaging studies of pattern separation typically leverage the repetition suppression effect (Grill-Spector et al., 2006), where the neural (here: BOLD) signal decreases in response to repeated stimuli compared to novel ones. Repetition suppression has been used to identify brain regions sensitive to changes in specific stimulus properties. If an area shows repetition suppression despite changes in the stimulus, it suggests insensitivity to the changed stimulus features. Conversely, no repetition suppression indicates sensitivity. This method also allows for plotting the curve of interference sensitivity when a parametric manipulation is used, which has led to the description of non-linear increases in activity as a function of lure similarity relative to repeats in the hippocampus (Motley & Kirwan, 2012) and CA3DG (Stark et al., 2013; Yassa et al., 2011), resembling the power function. More recently, studies using multivariate fMRI analysis methods corroborated the notion that the hippocampus reduces the representational overlap between interfering inputs, making even highly similar stimuli distinguishable and decodable (Berron et al., 2016; Chanales et al., 2017; Favila et al., 2016; Kyle et al., 2015; Wanjia et al., 2021). In sum, evidence from studies using both repetition suppression paradigms and multivariate pattern analysis converge on the hippocampus and the CA3DG region as key areas for mnemonic interference reduction.

Despite the evidence described above, there is some controversy around the existence (Quiroga, 2020), mechanisms (Aimone et al., 2011; Johnston et al., 2016), and behavioral measures (Deuker et al., 2014; Hunsaker & Kesner, 2013; Liu et al., 2016; Molitor et al., 2014) of hippocampal pattern separation in humans. An important aspect of the criticism is the meaningfulness of the used stimuli. Most tests of mnemonic discrimination rely on everyday objects or a varying arrangement of these in spatial scenes. Presenting participants with images of everyday objects could induce retrieval of already existing memory representations and confound pattern separation with pattern completion (Liu et al., 2016), or retrieval processes. Relatedly, this method cannot differentiate between the orthogonalization of incoming inputs (i.e., true pattern separation) and disparate voxel activity patterns due to partially overlapping, but

pre-existing engrams (Quiroga, 2020). Using never-before-seen, non-meaningful stimuli and investigating pattern separation signals at the time of encoding (Liu et al., 2016), could mitigate these concerns by limiting the activation of already available memories and prior associations.

In addition, recent work has emphasized the role of extra-hippocampal neocortical areas in conventionally applied mnemonic discrimination tasks (Amer & Davachi, 2023; Klippenstein et al., 2020; Nash et al., 2021). Specifically, it is suggested (Amer & Davachi, 2023) that interference resolution is promoted either by 1) allocating neuronal resources in accordance with task-demands, e.g., to suppress or enhance relevant information from sensory regions, or by 2) providing high-fidelity, distinct input to the hippocampus, and thus reducing the need for further separation. The frontoparietal network may play a key role in directing attention to unique features, and amplifying the separation of memory representations in the medial temporal lobe (MTL). In turn, cortical MTL areas have been suggested to be engaged in domain-selective interference reduction. The perirhinal cortex (PRC), which has rich connections with the ventral visual stream, is implicated in processing object information (Burke et al., 2014; Eacott & Gaffan, 2005), and has been found to be involved in the perceptual and mnemonic discrimination of complex objects in rats (Burke et al., 2014), primates (Bussey et al., 2002) and humans (Barense et al., 2010; Berron et al., 2018; Reagh & Yassa, 2014). The parahippocampal cortex (PHC), more connected to the dorsal visual pathway, is implicated in processing spatial relations (Eacott & Gaffan, 2005; Staresina et al., 2011) and resolving spatial-contextual interference (Berron et al., 2018; Reagh & Yassa, 2014). Importantly, not all human functional neuroimaging evidence supports domain-selectivity in the PHC and PRC. While some studies employing visual and mnemonic discrimination paradigms suggest that the engagement of these areas depends on representational content (Barense et al., 2010; Berron et al., 2018; Reagh & Yassa, 2014), others with similar designs did not find such specificity (Azab et al., 2014; Lawrence et al., 2020). Moreover, although the CA3DG is considered as a domain-general pattern separator (Azab et al., 2014), some have found higher activity in this area to object than spatial lures (Reagh & Yassa, 2014), which is inconsistent with the role of the hippocampus in spatial cognition (Goodrich-Hunsaker et al., 2008; Hartley et al., 2014) and spatial memory (Broadbent et al., 2004).

The goal of the current study was to assess the boundary conditions of domain-specific interference reduction in the PHC, PRC, and hippocampus. We opted for using complex unfamiliar items as stimuli in order to reduce the confounding effects of verbalization, semantic knowledge, and retrieval processes. We hypothesized that the PRC will be involved in object encoding, the PHC will be involved in spatial encoding, and the CA3DG will be engaged in interference reduction irrespective of the domain. Further, we hypothesized that the frontoparietal control network will be activated during both object and spatial lure discrimination, and that these regions will dynamically adapt their connectivity with occipital, medial temporal, and frontoparietal areas in order to resolve mnemonic interference.

To test mnemonic discrimination and its neuronal correlates in the object and spatial domain, we devised two old/new recognition memory tasks with non-meaningful fractal images. In the Object Task (Figure 1), we manipulated similarity of the within-item features (i.e., internal structure) between fractals, whereas in the Location Task (Figure 2), we manipulated similarity of the spatial position (i.e., the Euclidean distance) between fractals. We assumed that the within-item similarity and the spatial similarity of trials would induce interference in the two respective (object and spatial) domains. Here we report neuroimaging results from the encoding phase together with behavioral results from the recognition phase as pattern separation is a neural process supporting the encoding of unique episodes (Liu et al., 2016), the effect of which on behavior, i.e., memory discrimination, can be measured during recognition.

Results

Correct rejection of lures scales with similarity in both object and spatial domains

To assess the effect of similarity on recognition performance, we conducted a one-way repeated-measures ANOVA, which revealed differences in the ratio of "new" responses during the Recognition Phase as a function of trial type (target, lure, foil) in both tasks (Location: $F(2, 76) = 19.63$, $p < .001$, Object: $F(2, 76) = 264.99$, $p < .001$). We then compared the ratio of "new" responses between trial types directly with paired sample t-tests, and controlled for the false discovery rate (FDR) with the Benjamini-Hochberg method (Benjamini & Hochberg, 1995). All reported p values are adjusted accordingly, unless

otherwise stated. In the Object Task, post-hoc paired sample t-tests showed a significant difference between each combination of trial types (target - lure: $t(38) = -7.09$, $p < .001$, target - foil: $t(38) = -19.47$, $p < .001$, lure - foil: $t(38) = -16.63$, $p < .001$). In the Location Task, post-hoc paired sample t-tests showed a significant difference between target and lure trials ($t(38) = -4.39$, $p < .001$), and target and foil trials ($t(38) = -5.59$, $p < .001$), but not between lure and foil trials ($t(38) = -1.69$, $p = .099$). Importantly, the significant differences in the ratios of "new" responses between targets and lures, and targets and foils in both tasks demonstrated that participants discriminated between previously seen and changed trials, indicative of pattern separation.

Of note, foil trials in the Location Task were in fact analogous to lure trials (Figure 2b), but the fractals were presented further away from their original location (we defined fractals presented at least 450 pixels away from their original location as foils). The absence of a significant difference between foils and lures may indicate that this distance was not large enough for the fractal's position to be recognized as completely new, and thus failed to elicit a higher proportion of "new" responses. Following previous work with a two-response (old/new) version of the mnemonic discrimination task (Loiotile & Courtney, 2015; Stark et al., 2015), we replicated the above results using a signal detection measure of discriminability (d'). A d' between each pair of conditions revealed that the discriminability of all combinations of conditions was significantly higher than 0 in the Object Task (lure-target: $t(39) = 7.00$, $p < .001$, foil-lure: $t(39) = 15.12$, $p < .001$, foil - target: $t(39) = 16.47$, $p < .001$), and it was significantly higher than 0 between lures and targets ($t(39) = 4.29$, $p < .001$), and foils and targets ($t(39) = 5.2$, $p < .001$), but not foils and lures ($t(39) = 1.81$, $p = .078$) in the Location Task.

In the above analyses, we assigned the types target, lure and foil based on the similarity between the recognition trial and the first encoding trial in which the fractal was presented. However, as each fractal was presented twice during encoding (either in an exactly repeated or slightly changed version, see Figure 1a and Figure 2a), we hypothesized that the similarity between the recognition trial and the *second* presentation of the trial will also modulate participants' performance. In addition, the ANOVAs presented above disregard trial level similarity information. Therefore, in a follow-up analysis, we calculated the item and spatial similarity between each recognition trial and its first and second encoding presentation, and we assessed the relationship between each similarity measure and the probability of a "new" response

using binomial generalized linear mixed effects modeling with random intercepts (see Methods).

The probability of a "new" response in the Object Task was significantly associated with the first presentation item similarity ($p < .001$, Supplementary Table 1 - Model A) and the second presentation item similarity ($p < .001$, Figure 1c, Supplementary Table 1 - Model B). Adding both similarity measures to the model (Supplementary Table 1 - Model C) improved the fit significantly, and resulted in a slightly lower Akaike Information Criterion (AIC, Supplementary Table 2). In this model, only the effect of the similarity between the second presentation and the recognition trial remained significant ($p < .001$).

The probability of a "new" response in the Location Task was significantly associated with the first ($p < .001$, Supplementary Table 3 - Model A) and second ($p < .001$, Supplementary Table 3 - Model B) presentation's spatial similarity (Figure 2c). Adding both similarity measures to the model (Supplementary Table 3 - Model C) improved the fit, and resulted in a slightly lower AIC value (Supplementary Table 4). In this model, both the first presentation similarity ($p < .001$), second presentation similarity ($p = .006$), as well as their interaction ($p < .001$), were significantly associated with the probability of a "new" response.

Together, these behavioral results strongly suggest that mnemonic discrimination was affected by the similarity manipulation in both tasks. Moreover, not only the first, but the similarity of the second encoding trial influenced participants' behavior in both tasks. Therefore, we can conclude that participants paid due attention to the similarity information during the encoding phase, and the interference between the encoding trials provides a viable basis for assessing pattern separation at the neural level.

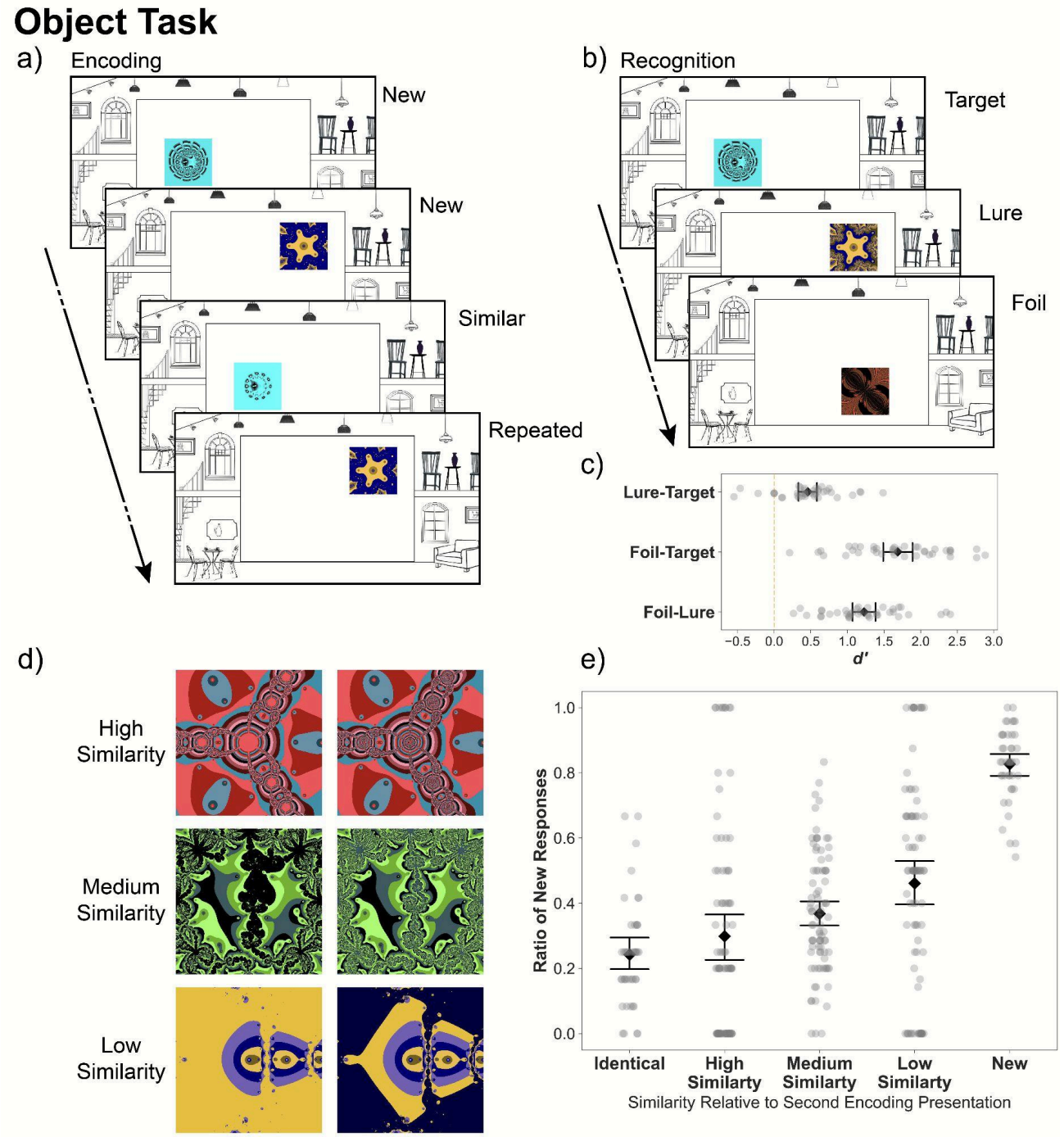

Figure 1. Object Task. Design, procedure, and recognition performance. a) The structure of the Object Task. During encoding, participants saw fractal images appear in an art gallery context (constant through the experiment) and were instructed to make aesthetic judgments about the images. Each trial lasted 3s, with jittered inter-trial intervals (0.5-8s). During recognition, participants had to judge whether they had seen exactly this fractal in the previous encoding phase. Trial duration was 4s with jittered inter-trial intervals (0.5-8s). b) Example pairs from each similarity bin used for the behavioral analysis. An independent sample of 30 participants rated each fractal pair on a scale of 0-9 (Identical - Very Different). c) The ratio of "new" responses is dependent on the similarity of lure fractals. The x axis depicts the similarity between the first presentation of the fractal type and the version presented at recognition. The y axis depicts the raw ratio of "new" responses for each participant. Error bars represent 95% confidence intervals.

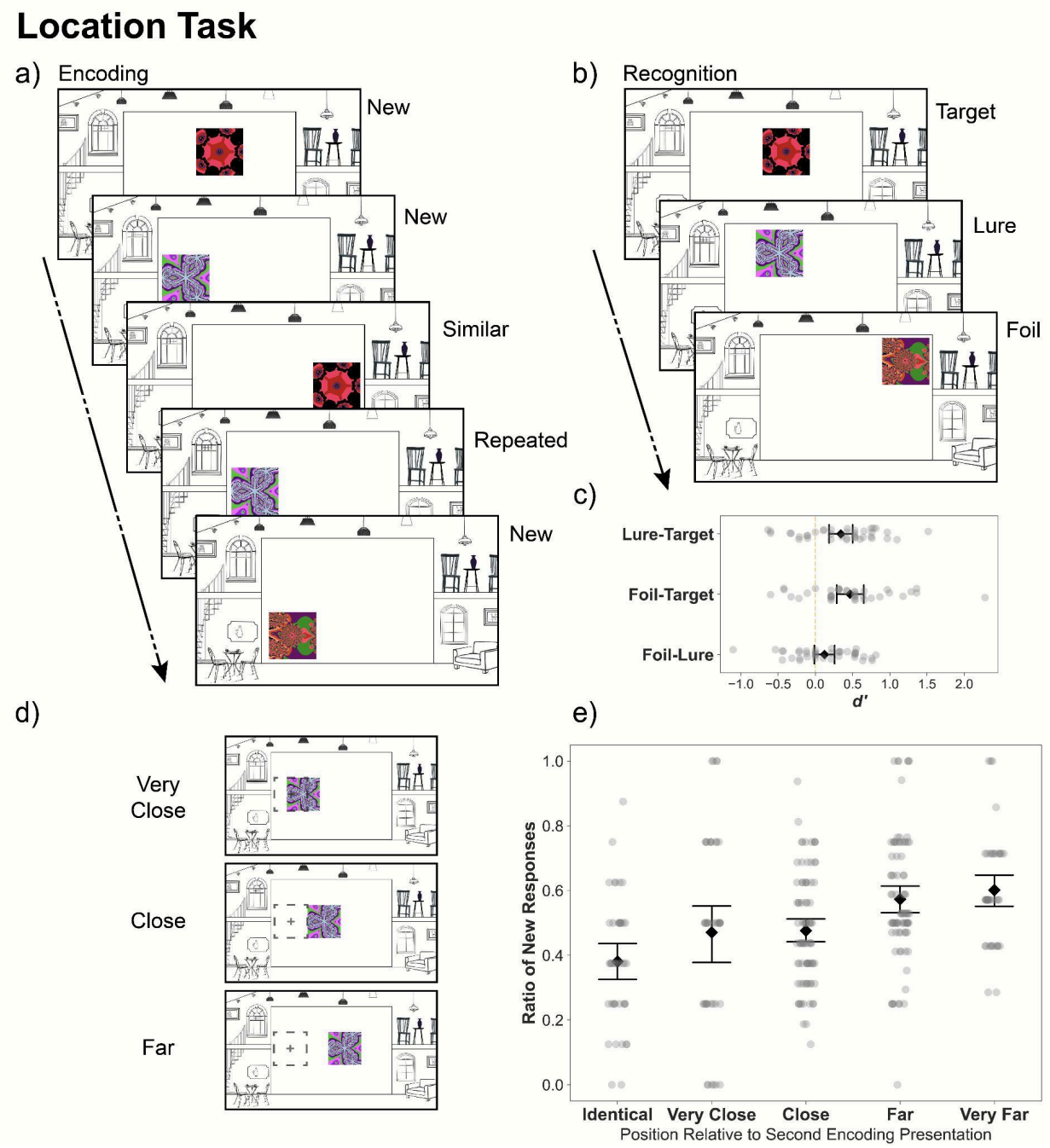

Figure 2. Location Task. Design, procedure, and recognition performance. a) The structure of the Location Task. During location encoding, participants saw fractal images appear in an art gallery context (constant through the experiment) and were instructed to make aesthetic judgments about the position of the images. Each trial lasted 3s, with jittered inter-trial intervals (0.5-8s). During recognition, participants had to judge whether they had seen the shown fractal at the exact current location in the preceding encoding phase. Trial duration was 4s with jittered inter-trial intervals (0.5-8s). b) Example pairs from each similarity bin used for the behavioral analysis. Very close pairs were presented 1-200 pixels away, close pairs were presented 200-400 pixels away, far pairs were presented 400-600 pixels away. Very far pairs are more than 600 pixels away from the second presentation. c) The ratio of "new" responses is modulated by distance. The x axis depicts the spatial similarity between the second presentation of the trial and the recognition trial. The y axis depicts the raw ratio of "new" responses for each participant. Error bars represent 95% confidence intervals.

Univariate fMRI signals during encoding highlight the role of neocortical areas in reducing interference between non-meaningful complex stimuli

Based on extant neuroimaging data, our prediction was that the CA3DG area as a domain general pattern separator will show repetition suppression to exactly repeated trials and increased BOLD signal to lure trials compared to repetitions. We expected the PRC and PHC to show this pattern (i.e., repetition suppression to repeats, and a relative increase to lures) in a domain-specific manner. First, we modeled the new, lure, and repeated encoding trials in a 2 (Presentation Rank: first vs second) - by - 2 (Trial Type: Lure vs. Repeat) design with four regressors (Figure 3a): first presentation of later repeats (Presentation 1, Type Repeat), first presentation of later lures (Presentation 1, Type Lure), repeats (Presentation 2, Type Repeat), and lures (Presentation 2, Type Lure). We opted for this balanced model to ensure that there are no baseline differences between the first presentations of later repeat and lure trials due to perceptual reasons. In a 2-by-2 repeated measures ANOVA, such an imbalance would be indicated by a main effect of Trial Type, while the strongest indicator of pattern separation would be an interaction between the Presentation Rank and Trial Type (Figure 3b). In cases where we had an a priori hypothesis regarding pattern separation in a given area (CA3DG and PRC in the Object Task, CA3DG and PHC in the Location Task), we used paired sample t-tests to directly assess whether activity is significantly lower for repeats than first presentation of later repeats, accompanied by activity to lures that is higher than activity to repeats. All reported p values, unless otherwise stated, are FDR adjusted per group of analysis (Benjamini & Hochberg, 1995), to account for multiple comparisons.

Object Task: Increased BOLD response to object lures compared to repetitions in the bilateral perirhinal cortex

In the Object task, a region-wise 2-by-2 repeated measure ANOVA revealed a main effect of Presentation Rank in the following regions: left CA3DG ($F(1, 38) = 5.79$, $p_{unadjusted} = .021$), left SUB ($F(1, 38) = 7.91$, $p = .026$), left PRC ($F(1, 38) = 16.07$, $p = .002$), and right PRC ($F(1, 38) = 25.35$, $p < .001$). The effect in the left CA3DG was not significant after adjusting for the FDR ($p_{adjusted} = .053$). The main effect of Presentation Rank was due to the lower

activity level at Presentation 2 compared to Presentation 1 in all regions, i.e. a repetition suppression effect. We did not find a main effect of Trial Type in any region, and thus we concluded that there was no baseline difference between the first presentations of different types. Notably, we did not find any significant effect in either the left or right PHC (all ps > .1), indicating that the experimental manipulations in the Object Task left the PHC largely unaffected. Based on our a priori hypothesis that the CA3DG and PRC are involved in object pattern separation, which should result in higher activity for lures than repeats, we directly compared the lure and repeat trials with paired sample t-tests in these areas. The difference between lures and repeats was not significant in either the left ($t(38) = 1.23$, $p = .271$) or right CA3DG ($t(38) = 1.55$, $p = .257$), however, it was significant in both the left ($t(38) = 2.51$, $p = .028$) and right ($t(38) = 2.34$, $p = .037$) PRC, suggesting that the PRC was sensitive to the similarity manipulation in object lure trials. We observed a strong repetition suppression to repeats relative to first presentation of repeats bilaterally in the PRC (left PRC: $t(38) = 3.26$, $p = .007$; right PRC: $t(38) = 3.8$, $p = .002$), but this comparison did not reveal a significant difference in the CA3DG (left CA3DG: $t(38) = 1.75$, $p_{unadjusted} = .089$; right CA3DG: $t(38) = 1.78$, $p_{unadjusted} = .083$).

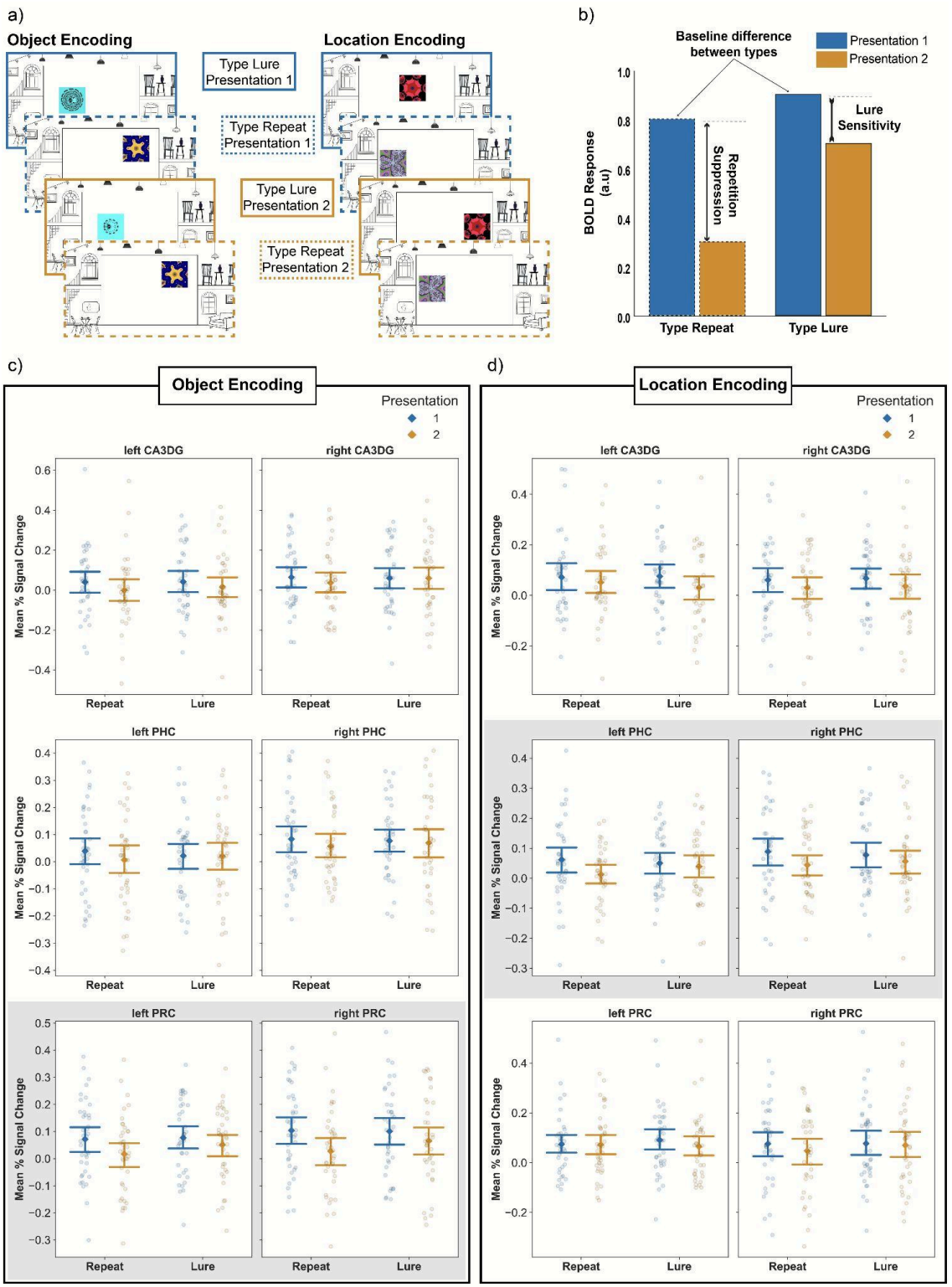

Figure 3. BOLD responses in the Encoding Phase modeled in a 2-by-2 design. a) First presentation trials were divided into first presentation of later lures and later repeats. b) Interpretation of results from the 2-by-2 model. c) Responses of the main medial temporal regions of interest during the object encoding. d) Responses of the main medial temporal regions of interest during location encoding. Neural response patterns in c) and d) suggesting differentiation between lure and repeat trials are shaded with gray. Abbreviations: CA3DG - CA3 and dentate gyrus, PHC - parahippocampal cortex, PRC - perirhinal cortex. Error bars represent 95% confidence intervals.

BOLD responses in PRC scale with object similarity

As a follow-up, we binned lure trials in the encoding into high- and low-similarity trials, which enabled us to analyze percent signal change as a function of similarity. For this analysis, we merged all first presentations into one explanatory variable, given that previously we did not find a baseline difference between the first presentations of different types. This resulted in four regressors of interest: Repeat, High-Similarity, Low-Similarity, and New trials. Item similarity level dependent activations from each region that showed a main effect of Presentation Rank in the previous balanced model were tested with a one-way repeated measures ANOVA. We found a significant effect of similarity in each region included in this analysis: left CA3DG ($F(3, 114) = 3.35$, $p = .022$), left SUB ($F(3, 114) = 3.96$, $p = .01$), left PRC ($F(3, 114) = 8.00$, $p < .001$), right PRC ($F(3, 114) = 12.04$, $p < .001$). Post-hoc comparisons revealed that low similarity lures elicited significantly higher activation than repeats in the bilateral PRC (left PRC: $t(38) = 2.43$, $p = .03$, right PRC: $t(38) = 3.2$, $p = .004$), and high similarity lures elicited marginally higher activation than repeats in the left PRC: $t(38) = 1.96$, $p_{unadjusted} = .057$ ($p_{adjusted} = .068$). No other areas expressed significant sensitivity to lure trials relative to repeats.

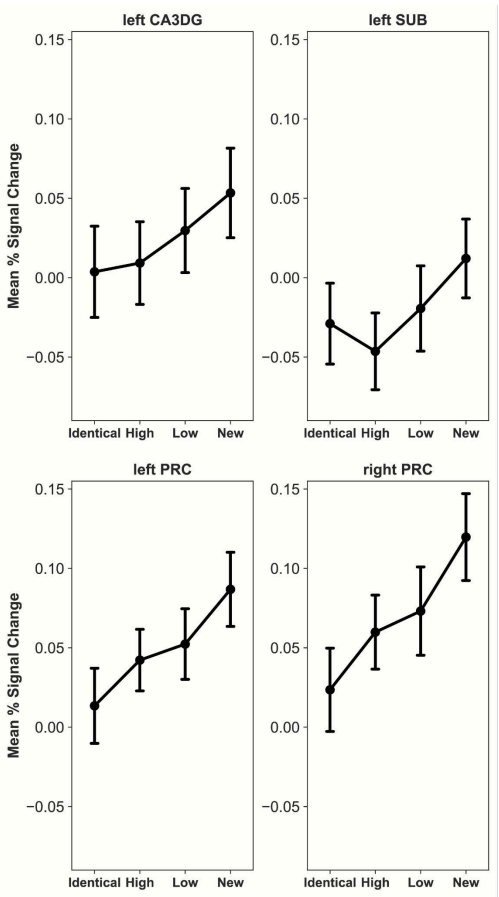

Figure 4. Similarity dependent activations during object encoding. The bilateral PRC expresses a significant increase to low similarity object lures. Responses from all areas that showed a significant effect in the previous 2-by-2 model were included in the figure. Abbreviations: CA3DG - cornu Ammonis 3 and dentate gyrus, SUB - subiculum,, PRC - perirhinal cortex. Error bars represent the standard error of mean.

Sensitivity of PRC to similarity predicts object mnemonic discrimination

To assess whether medial temporal lobe signals were related to participants' item discrimination performance, we first obtained the participant-specific slopes of sensitivity to item similarity from each region that showed any modulation by the Object Encoding conditions (left CA3DG, left SUB, left and right PRC). We achieved this by building linear mixed effects models, predicting each region's activity based on the level of similarity (Repeat, High Similarity, Low Similarity, New) with random slopes and random intercepts, and then extracted the participant-specific coefficients. Likewise, we used participant specific slopes of behavioral sensitivity to item similarity, obtained from linear mixed models predicting "new" responses based on the two similarity variables (between the first encoding presentation and recognition, and the second encoding presentation and recognition). We used Spearman correlations to assess the relationship between the neural and behavioral measures of item similarity sensitivity, and controlled for the FDR as before. Sensitivity of the right PRC correlated significantly with participants' behavioral sensitivity to the similarity between the second encoding trial and the recognition trial (r = 0.41, p = .035), indicating that the steeper the response of the right PRC was to increasing levels of similarity, the higher behavioral sensitivity the participant expressed to the similarity manipulation, which manifested as the probability of giving a "new" response to lure and new fractals.

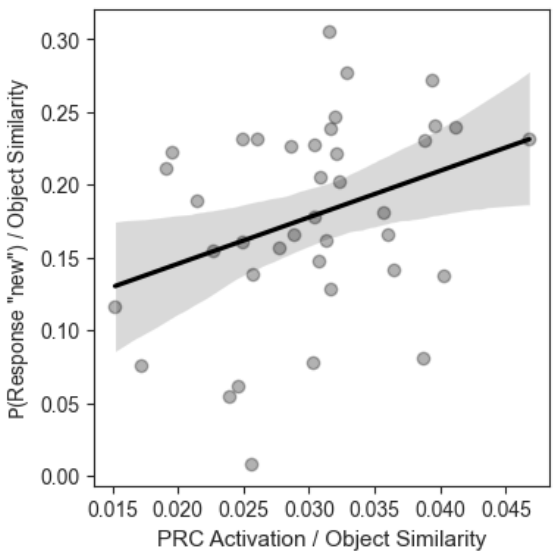

Figure 5. The association between the right PRC signal and mnemonic discrimination in the object domain. The behavioral sensitivity to object similarity - operationalized as the individual slope of similarity dependent "new" responses - correlates with the steepness of the right PRC's response to the level of similarity between object lures.

Location Task: No significant repetition suppression to spatial lures in the parahippocampal cortex

In the Location Task, a region-wise 2-by-2 repeated measure ANOVA revealed a main effect of Presentation Rank in the following regions: left CA1 ($F(1, 38) = 4.31$, $p_{unadjusted} = .045$), left CA3DG ($F(1, 38) = 8.53$, $p = .012$), right CA3DG ($F(1, 38) = 11.01$, $p = .008$), right SUB ($F(1, 38) = 10.85$, $p = .008$), left PHC ($F(1, 38) = 9.71$, $p = .009$), and right PHC ($F(1, 38) = 10.47$, $p = .008$). The effect in the left CA1 did not survive correction for multiple comparisons ($p_{adjusted} = .074$). The main effect of Presentation Rank was driven by a lower signal at Presentation 2 indicating wide-spread repetition suppression. In contrast, we found no effect in either the left or the right PRC (both ps > .1), suggesting that this area did not show repetition suppression during Location Encoding. We did not find a main effect of Trial Type in any region, and thus we concluded that there was no baseline difference between the first presentations of different types. Of note, the interaction between Presentation Rank and Trial Type in the left PHC was marginally significant ($F(1, 38) = 3.83$, $p_{unadjusted} = .058$, Figure 3c). Post-hoc paired sample t-test in the left PHC revealed that while activity was significantly higher for first presentation of later repeats than repeats ($t(38) = -2.8$, $p = .024$), there was no significant difference between first presentations of later lures and lures ($t(38) = -1.31$, $p = .236$). This pattern was also found in the right PHC (first presentation of later repeats vs. repeats: $t(38) = -2.87$, $p = .022$), first presentations of later lures vs. lures: $t(38) = -1.64$, $p = .163$). Activity was additionally significantly higher for lures than repeats in the left PHC ($t(38) = 2.22$, $p_{unadjusted} = .033$), but this effect did not persist after adjusting for multiple comparisons ($p_{adjusted} = .065$). We expected that the activation to lures would be higher than to repeats in the CA3DG, given its hypothesized role in pattern separation, however, the difference was not significant in either the left ($t(38) = -1.17$, $p = .301$) or right CA3DG ($t(38) = 0.4$, $p = .69$). We found repetition suppression to repeats relative to the first presentation of repeats in the right CA3DG ($t(38) = 2.06$, $p_{unadjusted} = .046$), which was not significant after adjusting for the FDR ($p_{adjusted} = .091$). Note, however, that the main effect of Presentation Rank in the bilateral CA3DG nonetheless indicates that the activity to lures and repeats was lower than to first presentations in this region.

High-similarity spatial lures tend to elicit increased activity in the left PHC

Next, we binned lure trials of the Location Encoding into high- and low-similarity trials to analyze percent signal change as a function of spatial similarity. Again, all first presentation trials were merged into one regressor, creating four similarity regressors: Repeat, High-Similarity, Low-Similarity, and New trials. In the statistical analysis of the extracted percent signal change values, we included all regions of interest that showed a response to the task manipulation in the previous analysis, i.e. left CA1, left and right CA3DG, right SUB, left PHC, and right PHC. Spatial similarity level dependent activations from each of these regions are shown in Fig 4. We assessed the sensitivity to spatial similarity in a one-way repeated measures ANOVA. We found a main effect of similarity in all regions included in this analysis (left CA3DG: $F(3, 114) = 4.24$, $p = .007$, right CA3DG: $F(3, 114) = 2.98$, $p = .034$, right SUB: $F(3, 114) = 3.17$, $p = .033$, left PHC: $F(3, 114) = 3.98$, $p = .01$, right PHC: $F(3, 114) = 2.93$, $p = .037$), except the left CA1 ($F(3, 114) = 2.17$, $p = .094$). Post-hoc comparisons revealed that the left PHC was the only area where the difference between repeated and highly similar trials was significant ($t(39) = 2.19$, $p_{unadjusted} = .035$), albeit this difference did not persist after adjusting for multiple comparisons ($p_{adjusted} = .104$).

The sensitivity of the right CA3DG to similarity is associated with spatial mnemonic discrimination

We then assessed the associations between the neural responses of the medial temporal ROIs and mnemonic discrimination in the spatial domain. For this purpose, we obtained the participant-specific slopes of sensitivity to spatial similarity from linear mixed effects models that predicted each region's responses based on the level of similarity. All regions that exhibited some modulation by the Location Encoding conditions were included in this analysis (left CA1, left and right CA3DG, right SUB, left PHC, and right PHC). Each participant's behavioral sensitivity (i.e. individual slope) to the spatial similarity between the first encoding presentation and the recognition trial, and the second encoding presentation and the recognition trial was used as a behavioral outcome. We ran Spearman correlations, and found an association between the right CA3DG response and the behavioral sensitivity to the similarity between the second encoding trial and the recognition trial ($r = 0.34$, $p_{unadjusted} = .034$, Supplementary Figure 1) that did not remain significant after adjusting for the FDR ($p_{adjusted} = .168$).

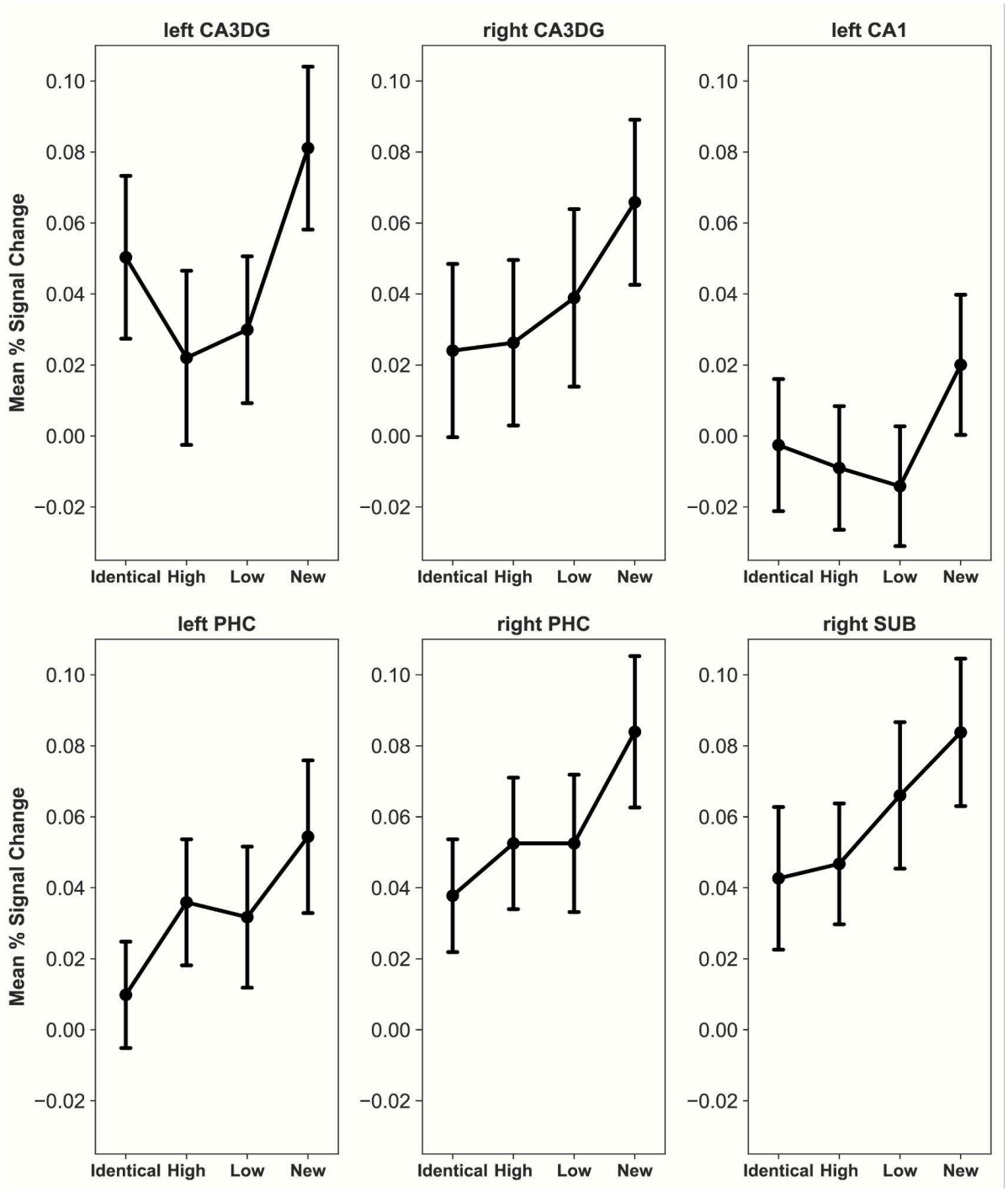

Figure 6. Similarity dependent activations during location encoding. The left PHC expresses a significant increase to high similarity spatial lures. Responses from all areas that showed a significant effect in the previous 2-by-2 model were included in the figure. Abbreviations: CA1 - cornu Ammonis 1 and 2, CA3DG - cornu Ammonis 3 and dentate gyrus, SUB - subiculum,, PHC - parahippocampal cortex. Error bars represent the standard error of mean.

Task-dependent responses to similarity in the parahippocampal and perirhinal cortex

Next, we tested whether the activity of PRC and PHC statistically differed depending on the task context, i.e., whether the PRC is more engaged in object interference resolution than the PHC and vice versa. To this end, we merged data from the two tasks and two regions, and conducted a repeated measures ANOVA with area (PHC versus PRC), hemisphere, similarity level (Repeat, High Similarity, Low Similarity, New), and task (Object versus Location) as within-subject factors. We found a significant main effect of similarity level ($F(3, 114) = 13.07$, $p < .001$), and a main effect of hemisphere ($F(1, 38) = 13.07$, $p = .043$). The main effect hemisphere was due to higher mean percent signal change in the right hemisphere ($t(623) = 4.08$, $p < .001$). We did not find a main effect of either task ($F(1, 38) = 0.01$, $p = .922$) or area ($F(1, 38) = 1.28$, $p = .266$). Importantly, the analysis revealed a significant three-way interaction between similarity level, area, and task ($F(3, 114) = 3.87$, $p = .011$). This interaction indicates that depending on the task context – and thus the type of information that needed to be attended – similarity induced interference differentially modulated the activity of the PRC and PHC (Figure 7).

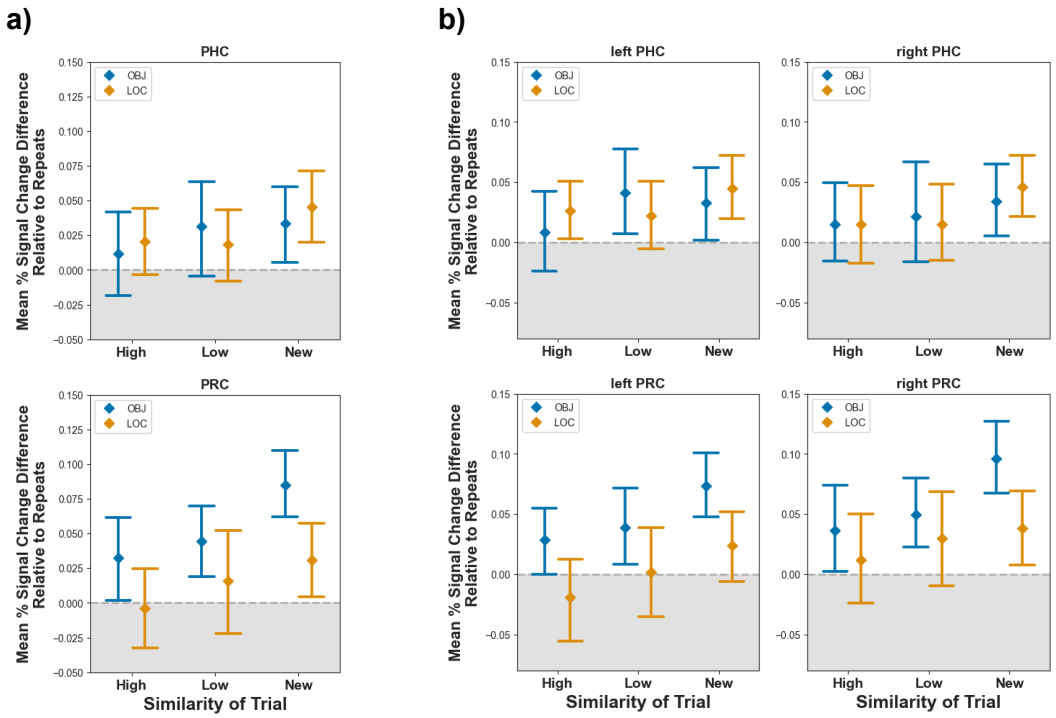

Figure 7. Similarity level dependent responses of the parahippocampal and perirhinal cortices across the two tasks. Responses to repeats were extracted from the mean % signal change values of each similarity level. Values around and below 0 therefore can be considered repetition suppression. Panel a) shows the cross-hemisphere average, and panel b) shows the signal from each hemisphere. A three-way interaction between similarity-level, task and area signifies that similarity dependent responses differ based on task context. Error bars represent 95% confidence intervals.

The frontoparietal control network is activated by both spatial and object lures

Recent work highlighted the potential role of the frontoparietal control network in mnemonic discrimination. In a series of analysis, we aimed to test 1) whether these areas are recruited when viewing spatial and object lures of non-meaningful images, 2) whether the connectivity of the frontoparietal network increases during the encoding of lure trials, and 3) whether the frontoparietal network interacts with the medial temporal regions of interest to achieve mnemonic discrimination.

In a whole brain analysis, we modeled new, lure, and repeated encoding trials in a 2-by-2 design with four regressors as above (Figure 3a), separating the first presentation of later lures and of later repeats into two regressors. Following previous work (Nash et al., 2021; Reagh & Yassa, 2014), we chose the contrast *lures - first presentation of later lures* as our comparison of interest to identify areas that show high activity to lures, disregarding the visual features they share with first presentations and tapping on mnemonic processes. Results from the contrast (*lures - first presentation of later lures*) > (*repeats - first presentation of later lures*) are reported in Supplementary Table 4 and 5.

We found 13 clusters in the Object Encoding (Figure 8a) and 12 clusters in the Location Encoding (Figure 8b) that showed significantly higher activity to lures than their first presentation, summarized in Supplementary Table 6 and 7. Importantly, the clusters derived from the Location and Object task moderately overlapped (Dice-Sørensen coefficient = 0.54, Figure 8c), and both covered regions belonging to the frontoparietal control network, i.e., the middle frontal gyrus, the angular gyrus, and the supramarginal gyrus (Dixon et al., 2018; Uddin et al., 2019). No significant clusters were found in the medial temporal lobe.

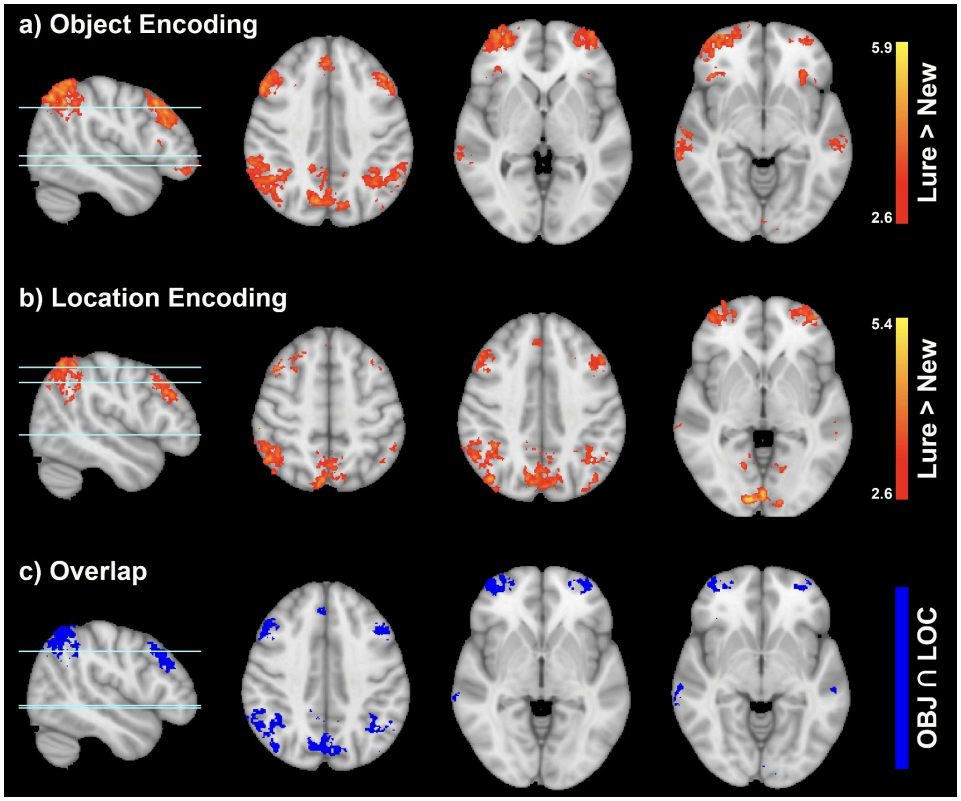

Figure 8. Clusters of significant activation to Lures > First trials. Whole brain activations to lure - first presentation trials showed a high overlap between the Object and Location Tasks. Frontoparietal regions were activated by both task contexts. a) Significant clusters of activation during the Object Encoding. b) Significant clusters of activation during the Location Encoding. c) Overlap of significant clusters in the Location and Object Tasks.

Functional connectivity of the frontoparietal attention network strengthens in response to spatial and object lures

Next, we tested how the connectivity of the frontoparietal network changes during lure discrimination. We selected three frontoparietal areas per hemisphere that emerged consistently across the two tasks during lure trials in the whole-brain analysis (the angular gyrus, the supramarginal gyrus, and the middle frontal gyrus) to serve as seeds in the generalized psychophysiological interaction analyses (gPPI, McLaren et al., 2012). Psychophysiological interaction (PPI) analysis examines task-specific modulations of the functional connectivity of an area (Di et al., 2021; Friston et al., 1997) by modeling the interaction between the timeseries of the area (physiological variable) and a task condition (psychological variable). In a gPPI analysis, in contrast to the standard PPI approach, each task condition and its interaction with the physiological variable is modeled, thus covering the entire experimental space, leading to better model fit (McLaren et al., 2012). Accordingly, our gPPI models included a regressor for each task condition and the interaction between the seed activity and task condition. First we report results from each seed region's interaction with the lure condition (lure PPI contrast), which reflects increases in connectivity relative to the baseline. Cluster

statistics for the lure PPI contrast can be found in Table 1 (Object Task) and Table 2 (Location Task). Second, we report results from the contrast lure PPI > repeat PPI which indicate if the seed region interacts with some areas more in the lure condition than the repeat condition.

In the Object Task, only the right angular gyrus and the right middle frontal cortex seeds expressed increased functional connectivity with other regions. We found 1 cluster (256 voxels, max. z = 3.42, p = .044) of increased connectivity during the encoding of object lures between the right angular gyrus seed and the left supramarginal gyrus and left angular gyrus. The right middle frontal gyrus seed increased its connectivity with two clusters: one located in the left angular cortex (301 voxels, z = 3.5, p = .011), and the other in the posterior region of the middle temporal gyrus (343 voxels, z = 3.64, p = .004). No significant clusters were found for the contrast lure PPI > repeat PPI in the Object Task.

Table 1. Significant clusters in the Object Task for the lure PPI contrast

Seed region	Areas in cluster	N. voxels	Max. z	Cluster p
right angular gyrus	left supramarginal gyrus, left angular gyrus	256	3.42	.044
right middle frontal gyrus	left angular gyrus	301	3.5	.011
	left middle temporal gyrus	343	3.63	.004

In the Location Task, we found enhanced functional connectivity between the left angular gyrus seed and the right frontal pole, right supramarginal gyrus, right postcentral gyrus, and right angular gyrus during the encoding of spatial lures. The left supramarginal gyrus increased its connectivity with the right frontal pole and superior frontal gyrus, right middle temporal gyrus, bilateral cingulate and precuneus cortex, right angular and supramarginal gyrus, and left lateral occipital cortex. The right supramarginal gyrus expressed a similar, but even more extensive pattern of connectivity increase, involving some additional sensory areas, such as the lingual gyrus and occipital fusiform cortex, in addition to bilateral frontal and parietal regions. As for the left middle frontal gyrus seed, only two significant clusters of connectivity increase

were found, one in the right frontal pole and one in the right angular gyrus. No significant connectivity increase was found for the right angular gyrus and right middle frontal gyrus seeds for the lure PPI contrast.

Table 2. Significant clusters in the Location Task for the lure PPI contrast

Seed region	Areas in cluster	N. voxels	Max. *z*	Cluster *p*
left angular gyrus	right angular gyrus, supramarginal gyrus	383	3.33	.002
	right frontal pole	373	2.92	.002
	right postcentral gyrus and supramarginal gyrus	282	3.05	.023
	right supramarginal gyrus	266	3.82	.037
right angular gyrus	left angular gyrus, left supramarginal gyrus	256	3.42	.044
left supramarginal gyrus	right angular gyrus	2055	3.69	< .001
	right frontal pole	1141	3.62	< .001
	right middle temporal gyrus, posterior division	931	3.91	< .001
	right posterior cingulate and precuneus	899	3.3	< .001
	left lateral occipital cortex	426	3.44	< .001
	left precuneus	296	3.3	.013
	right superior frontal gyrus and frontal pole	259	3.55	.037
right supramarginal gyrus	right angular gyrus and lateral occipital cortex	3016	3.68	< .001
	left frontal pole	1607	3.56	< .001
	right middle temporal gyrus, posterior division	1455	3.47	< .001
	bilateral lingual gyrus	1300	3.81	< .001
	right frontal pole	1087	3.99	< .001
	left inferior and middle frontal gyrus	1056	3.72	< .001
	right middle frontal gyrus	845	4	< .001
	left middle frontal gyrus	589	4.14	< .001
	right middle frontal gyrus, precentral gyrus	549	3.1	< .001
	bilateral precuneus	476	3.2	< .001

	right fusiform gyrus	426	3.37	< .001
	bilateral paracingulate gyrus	413	3.55	< .001
	right superior frontal gyrus	405	3.33	< .001
	bilateral posterior cingulate gyrus	402	3.43	< .001
	left lingual gyrus, left fusiform gyrus	372	3.54	.002
	left paracingulate gyrus, left anterior cingulate gyrus	355	3.39	.002
	left lateral occipital cortex, left angular gyrus	350	3.59	.003
	left orbitofrontal cortex	331	3.44	.005
	right lateral occipital cortex	315	3.36	.007
	right middle temporal gyrus, anterior division	304	3.13	.01
left middle frontal	right frontal pole	467	3.09	< .001
	right angular gyrus, right supramarginal gyrus	328	3.41	.005

Additionally, we found two significant, anatomically overlapping clusters for the lure PPI > repeat PPI contrast in the Location task. Both the left supramarginal gyrus (363 voxels, max. z = 3.79, p = .001) and the right middle frontal gyrus (23 voxels, max. z = 3.5, p = .006) increased their connectivity with the left occipital pole during lure encoding, and this increase was significantly higher than that in the repeat condition.

These results clearly indicate that the frontoparietal network was recruited during the encoding of spatial and object lures. Specifically, both the inter- and intra-connectivity of the network increased in response to similar trials, suggesting enhanced communication within the network and modulation of downstream regions.

Connectivity between the supramarginal gyrus and medial temporal regions at encoding influences recognition performance

To examine the connectivity specifically between the frontoparietal ROIs and our main medial temporal ROIs, we extracted the preprocessed and motion corrected mean timeseries data using anatomical masks of the left and right CA3DG, PHC, PRC, angular gyrus, supramarginal gyrus, and middle frontal gyrus, and created one correlation matrix per task for each subject. Each medial temporal ROI exhibited significant connectivity with the frontoparietal regions in both tasks (Supplementary Figure 3 and

4). Further, the connectivity between the right PHC and the left supramarginal gyrus was significantly higher during the Location Encoding than the Object Encoding ($t(39) = 2.23$, $p = .025$), but this difference was not significant after adjusting for the FDR ($p_{adjusted} = .521$). No other difference was found in the connectivity of medial temporal and frontoparietal regions between the two tasks (Figure 9).

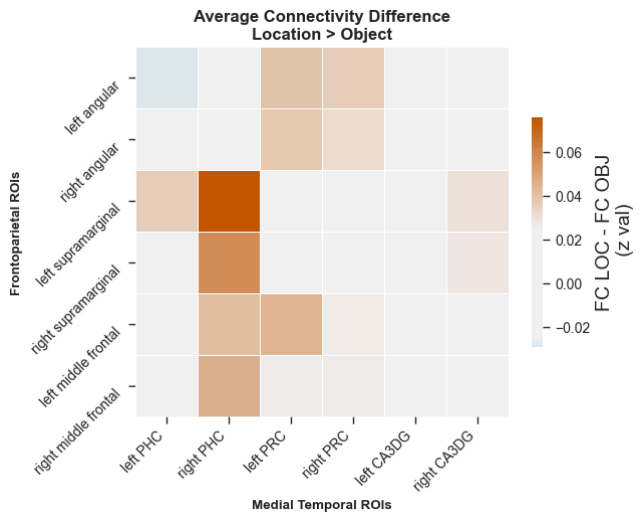

Figure 9. Functional connectivity differences between the Object and the Location Encoding. The connectivity between the right PHC and left supramarginal gyrus was higher during Location Encoding than Object Encoding. The correlation between each medial temporal ROI and each frontoparietal ROI during the Object Encoding was subtracted from the Location Encoding for the purpose of visualizing the differences in connectivity between the tasks.

We then proceeded to assess the associations between the medial temporal - frontoparietal connectivity and behavior. We correlated the behavioral variables of object and spatial similarity sensitivity with the connectivity between each medial temporal ROI and frontoparietal ROI. Intriguingly, we found exclusively negative relationships between the connectivity of both the PHC and PRC during encoding and the behavioral sensitivity to similarity. Due to the number of comparisons (36 connectivity variables), none of the correlations remained significant after FDR adjustment. We report these associations in order of effect size in the supplementary. Of interest, in the Object task the sensitivity to the similarity between the first encoding presentation and the recognition trial was associated with the connectivity between the right PRC and right angular gyrus ($r = -0.41$, $p = .01$). The sensitivity to the similarity between the second encoding presentation and the recognition trial was associated with the connectivity between the right PHC and left supramarginal gyrus ($r = -0.41$, $p = .009$), and the left PRC and right supramarginal gyrus ($r = -0.41$, $p = .009$). In the Location task the associations were weaker, but also exclusively negative, and included both the PRC and PHC connectivity (see Supplementary Table 9). We found no associations between the behavioral measures and the connectivity of the CA3DG in either task. Taken together, these results provide evidence that the connectivity

between the medial temporal and frontoparietal regions were relevant for participants' mnemonic discrimination performance, but this effect was not domain-specific, i.e., both the PRC and PHC connectivity was related to behavior.

Discussion

The present study investigated the effects of interference on neuronal activity in the human hippocampus, perirhinal cortex, parahippocampal cortex, and frontoparietal control network in two information domains that were previously found to be processed via independent pathways in the medial temporal lobe: object features and spatial information. We believe our results provide three important contributions to the cognitive neuroscience of memory. First, amid the debate about the anatomical and functional independence of the two medial temporal pathways (Burke et al., 2018; Connor & Knierim, 2017; Lawrence et al., 2020; Nilssen et al., 2019; Rolls, 2024), our results support the notion that the perirhinal and parahippocampal cortices contribute complementary information about individual items and their spatial context, respectively. Second, we demonstrate that the perirhinal and parahippocampal cortices, but not the CA3DG, show a sensitivity to interfering mnemonic information, when this information is not easily verbalized and categorized. This finding does not align well with the view that the CA3DG area is the primary locus of pattern separation, or that representational repulsion takes place in the CA3DG even when the overlap in input does not require it. Third, we found evidence that frontoparietal network regions are recruited in response to both spatial and object interference, and the connectivity of these regions flexibly changes according to task demands. Below we discuss some probable explanations for these results, and place them within a general discussion on medial temporal lobe function and human memory.

Content-specific pathways in the medial temporal lobe

Anatomical studies in both rats and primates point to a potential functional specialization, as most inputs to the PRC originate in the object-based ventral visual stream, while the PHC (called postrhinal cortex in rodents) receives its input mainly from the more spatial dorsal processing stream (Burwell & Amaral, 1998a, 1998b). A

double dissociation in these regions' functionality was also supported by lesion (Eacott & Gaffan, 2005; Gaffan et al., 2004) and human neuroimaging studies (Staresina et al., 2011). Recently, however, the independence of the two medial temporal pathways was called into question by some contradictory findings on the functional specialization of these areas (Burke et al., 2018; Lawrence et al., 2020) and a reevaluation of the anatomical data (Nilssen et al., 2019).

In line with prior fMRI work in domain-specific mnemonic processing (Bencze et al., 2024; Berron et al., 2018; Reagh & Yassa, 2014), our results support the view that a division of labor exists between the PRC and PHC according to object and spatial features. We found that the PHC was affected by the experimental manipulations of locations, i.e., it showed strong repetition suppression to repeated trials viewed in unchanged locations, and we found some tentative evidence that its activity was modulated by high-similarity spatial lures. At the same time, we did not find a significant repetition suppression effect during location encoding in the PRC, which suggests no perceptual memory representation for location information in this area. On the other hand, the experimental manipulations of object features elicited significant effects in the PRC, including repetition suppression to repeated trials, and activity changes as a function of similarity. A direct comparison of the effects of similarity on the PRC and PHC in the Object and Location Task revealed a three-way interaction of similarity, area, and task, demonstrating that the responses of these areas differed based on task context. Notably, new and repeated trials had an identical structure during the location and object encoding phases, yet the PRC and PHC showed sensitivity to the task context, and only expressed repetition suppression when the task demands matched their respective specialization, i.e. processing object features or spatial information, suggesting that PRC/PHC responses were not modulated solely by trial features, but top-down control processes based on task demands.

Neural responses in medial temporal neocortical areas are modulated by small alterations in non-meaningful stimuli even when the hippocampus shows repetition suppression

Besides the differences in the expression of repetition suppression, the PRC and PHC also showed sensitivity to highly interfering trials in accordance with their task

domains. Specifically, in the Object Task we found that lure trials elicited significantly higher activation than repeated trials in both the left and right PRC. Moreover, the sensitivity of the PRC to object lure similarity was related to participants' mnemonic discrimination behavior. Correspondingly, in the Location Task we found a tendency of high similarity lure trials to elicit higher activation than repeated trials in the left PHC. When considered together with the result that the activation to lure trials did not differ statistically from first presentation trials in either the left or and right PHC, this suggests that the PHC was sensitive to interfering location information.

The CA3DG, on the other hand, did not express any significant increase in response to lure trials in either task. The results from the two tasks together indicate that the activity of neocortical areas in the medial temporal lobe may be modulated by high-interference trials even when the CA3DG exhibits repetition suppression, suggesting the integration of non-meaningful stimuli in the hippocampus and their differentiation in the neocortex.

Numerous previous studies found evidence that the dentate gyrus is involved in creating unique memories in humans (e.g., Azab et al., 2014; Bakker et al., 2008; Berron et al., 2016; Kyle et al., 2015), and some have even argued for a necessary role of the dentate gyrus in mnemonic discrimination (Baker et al., 2016; Mitchnick et al., 2024). A key difference between preceding work and ours is the meaningfulness of stimuli used. Outside of the pattern separation literature, the relevance of meaningfulness has been demonstrated in a range of fields including perceptual decisions (Barense et al., 2011), working memory (Asp et al., 2021; Williams et al., 2023) and episodic memory (Bartlett, 1995; Brady et al., 2019; A. G. Goldstein & Chance, 1971; Wiseman & Neisser, 1974). A few studies investigating pattern separation used novel, non-meaningful stimuli, and found evidence of hippocampal involvement, but these studies either included items that resembled real objects and were verbally labeled (Duff et al., 2012), or they required only perceptual (Mitchnick et al., 2022) or working memory discrimination (Paleja et al., 2014), rather than long-term mnemonic discrimination. To the best of our knowledge, this is the first study to examine how interfering, non-meaningful stimuli are encoded in long-term memory by the CA3DG with an explicit instruction to remember the details of the experience (cf. Brickman et al., 2014).

Relation to theories of memory in the human MTL

The apparent domain-wise specialization of the PRC and the PHC, and the lack of a pattern-separation signal to non-meaningful stimuli in the CA3DG, broadly align with a representational account of the medial temporal lobe. According to this account, areas are not specialized in terms of the type of computation they carry out, but rather according to the type of information they process, e.g. object versus space, high- versus low-dimensional content (Cowell et al., 2019; Martin & Barense, 2023). Advocates of this account see a continuity between the visual and memory systems (Barense et al., 2005; Martin & Barense, 2023; Yonelinas, 2013), with the complexity of representable information gradually increasing from the early visual cortex to the hippocampus. It may be that the presented fractals did not elicit pattern separation in the hippocampus as images of everyday objects normally do because these stimuli were unfamiliar to participants and thus were comparably lacking in contextual and meaningful features, and as a result were still lacking in complexity compared to everyday objects. One interpretation of our results is that only experiences that differ in meaningful features are encoded in long term memory by the CA3DG in a pattern separated fashion. This interpretation still allows for the possibility that hippocampal pattern separation mechanisms underlie perceptual or working memory discrimination of non-meaningful complex objects, as suggested by recent research (Mitchnick et al., 2022; Paleja et al., 2014).

Even though the fractal objects were visually complex and the nature of the tasks required binding between spatial locations and objects, the dimensionality of the stimuli was below those of meaningful images, which can be ascribed multiple semantic features as well as personal associations. For example, an image of a dog can be placed along dimensions of perceptual features, e.g., the color and luminosity of each pixel, and along semantic dimensions as well, such as the biological attributes of the species *Canis familiaris*, or emotions we associate with them. Along these lines, our results do not provide evidence against the view that there is no pattern separation in the human hippocampus (Quiroga, 2020), at least in the strict sense of the term as an orthogonalizing operation or 'repulsion' of representations, and it is simply the difference between existing and partially overlapping representations that leads to distinguishable activity between lures and repeats. Since the fractals presumably activated no or very few existing associations, no significant difference could be

detected between repeats and lures. Future studies may shed light on whether making participants more familiar with such non-meaningful stimuli, and assigning meaning and associations to them, may facilitate pattern separation in the hippocampus.

Frontoparietal network involvement in interference reduction

We found evidence that the frontoparietal network is activated during the encoding of lure trials irrespective of domain (space vs. object), and its connectivity increases within the network and with downstream sensory regions such as the lateral occipital cortices, when interference resolution is necessary. We interpret this as a regulation of regions that process sensory information in order to either emphasize or downplay differences during the encoding of lures. These data alone cannot disambiguate, however, whether the connectivity increase facilitated the integration or differentiation of interfering information in this context.

The whole-brain gPPI analysis did not provide evidence that connectivity with either the hippocampus, the PHC, or the PRC changed during lure encoding in either task. This could be related to either the relatively low power of PPI methods for fMRI data (Di & Biswal, 2017; J. X. O'Reilly et al., 2012), the lower signal-to-noise ratio in the medial temporal area, the small volume of these regions, or a stable connectivity profile between the MTL and the frontoparietal areas, which did not change significantly throughout the experiment. It is important to emphasize that the direction and amount of influence of the frontoparietal regions over sensory and medial temporal regions may not be directly translatable into changes in functional connectivity, and influence could also be exerted over stable connectivity, which led us to examine the region-to-region connectivity specifically between the medial temporal and frontoparietal ROIs.

Our region-to-region connectivity analysis between medial temporal and frontoparietal seeds confirmed functional connectivity between these networks. Further, we found tentative evidence that the connectivity between the PHC changed according to task context, as the right PHC displayed higher connectivity with the left supramarginal gyrus during location encoding than object encoding. However, no other differences were found in the connectivity patterns of the two tasks. The associations between the medial temporal - frontoparietal connectivity and recognition performance further suggest that the synchronicity of these areas carries behavioral relevance. The fact that the correlations between behavioral sensitivity to similarity and the strength of

functional connectivity between the medial temporal and frontoparietal regions were negative may imply that the connectivity contributed to the integration of interfering information, rather than to differentiation, enabling the second encoding presentation to modify the existing representation of the first encoding trial with an integrated representation over the trials. Previously, suppression of competing memory patterns in ventral visual areas by the lateral prefrontal cortex has been shown to lead to adaptive forgetting of interfering information (Wimber et al., 2015), and numerous studies demonstrated the role of the dorsolateral prefrontal cortex in reducing interference by retrieval suppression and inhibitory control (Anderson et al., 2004; Anderson & Hulbert, 2021; Depue et al., 2016). Based on these findings, it may be that the medial temporal - frontoparietal connectivity indicated the suppression of competing information, which in turn led to the decreased sensitivity to similarity. Altogether, these results clearly indicate an involvement of the frontoparietal network during lure discrimination, however, we have so far limited evidence regarding whether and how the frontoparietal network interacts with medial temporal regions to achieve interference resolution.

Limitations and future directions

One important limitation of our approach is the fact that we analyzed data from the CA3 and dentate gyrus areas as a single unit. Given the role of CA3 in pattern completion, one might argue that the activity pattern we see in the CA3DG is the result of pattern completion in the CA3, suppressing the pattern separation signal in the dentate gyrus. At the time of writing this work, there is no published valid and reliable method of delineating these two critical subfields on 3T MRI data. In collapsing the two subfields, we have followed a substantial body of previous fMRI studies that nonetheless found a pattern separation signal in this combined region of interest, albeit using everyday objects as stimuli (e.g. Dimsdale-Zucker et al., 2018; Klippenstein et al., 2020; Nash et al., 2021; Reagh & Yassa, 2014; Yassa & Stark, 2011).

Although ideally the CA3 and dentate gyrus subregions should be certainly studied separately, several factors underscore the validity of our results. First, a repulsion-like process has been reported in previous studies that used a combined CA3DG ROI, in which hippocampal pattern separation went beyond orthogonalizing inputs, i.e., the representation of overlapping inputs became less similar than non-overlapping inputs (Chanales et al., 2021; Favila et al., 2016). Second, depending on

task demands, the CA3 is also expected to contribute to pattern separation, and neurons engaged in pattern separation compatible behavior are found in the proximal parts of the CA3 (GoodSmith et al., 2019; Lee et al., 2020). Nonetheless, in our study we identified activity patterns consistent with the differentiation between repetitions and interfering lures in the PRC and PHC but not the CA3DG; irrespective of whether the source of this signal is in the CA3 or dentate gyrus. We nevertheless hope that future studies will elucidate this detail when a validated protocol of DG segmentation is available, and we can learn about the dynamics of pattern separation in both the CA3 and dentate gyrus - potentially through the reanalysis of this dataset as well.

Our conclusions regarding the extent of domain-selective functional specialization in the medial temporal lobe are limited by not interpreting data on the entorhinal cortex. Numerous previous studies suggested that the anterolateral entorhinal cortex is engaged in object processing, and the posterior medial entorhinal cortex is engaged in spatial processing (Berron et al., 2018; Knierim et al., 2014; Reagh & Yassa, 2014), and functional connectivity results seem to support these regions' differential attachments to the object and spatial pathway (Maass et al., 2015). Unfortunately, the low signal-to-noise ratio in this area in our fMRI data made it infeasible to draw any conclusions about domain-specific processing in the EC, let alone separate its two subregions. Being situated between the PRC, PHC, and hippocampus, and providing a gateway to the CA3DG, it is an interesting question how much sensitivity the entorhinal cortex would show to object and spatial lures of non-meaningful stimuli. Future neuroimaging work, with acquisition parameters better suited to study this area so susceptible to signal drop-out and distortions, should shed light on the domain-selectivity of the anterolateral and posterior medial parts of the entorhinal cortex.

Concluding remarks

Our work critically revisits the question of pattern separation in the CA3DG and domain-dependent interference reduction in the medial temporal neocortex using the repetition suppression paradigm for fMRI data. We replicated findings on content-specific processing in the medial temporal lobe with novel, non-meaningful stimuli, which serves as an important contribution to the discussion on the functional organization of the human medial temporal lobe. Outside of the medial temporal lobe,

we found evidence that the frontoparietal network is engaged during lure encoding irrespective of representational domain which manifested in the whole-brain activation to lure trials as well as an increase in functional connectivity in response to lures. Our results present potential initial evidence that frontoparietal-medial temporal connectivity regulates mnemonic discrimination. Further, contrary to our expectations, we found that the CA3DG responds with repetition suppression to interfering stimuli which contradicts previous accounts of pattern separation in this area. These results advance our understanding of how unique memories are created by a widespread collaboration of brain areas, and raises the intriguing question where the limits of hippocampal pattern separation lie.

Materials and Methods

Participants

Power analysis based on pilot behavioral data and conducted with the software GPower indicated a sample size of 40 participants needed to show the behavioral effects of the similarity manipulations at 95% statistical power. Forty-six healthy volunteers (25 female, 21 male, 20–30 years old) were recruited for the study from the local student community. All participants were screened for psychiatric or physical illness, metal implants and current medications. The study was approved by the Ethical Committee of the Medical Research Council, Hungary (ethics approval number: OGYÉI/28291-2/2020), and was carried out in accordance with the code of ethics for human experiments (Declaration of Helsinki). Participants gave written informed consent, and they received either monetary compensation or course credit for their participation. Data of five participants could not be used for the analysis because of technical issues in the MRI (n=3), unfinished data acquisition (n=1), and missing log files due to experimenter error (n=1). Two participants were excluded due to incidental neurological findings. The final sample included 39 participants (19 female, 20 male, 20–30 years old with mean age of 22.61 years and standard deviation of 2.36 years).

Stimuli

The art gallery framing was created by combining drawn images of furniture and plants freely available on the internet. Fractal images (in size 300 * 300 pixels) were generated using Python 3.7.3 by applying the Newton-Raphson method to finding the roots of polynomials and transcendental functions. We created 181 fractal types, each defined by a unique function, and 3 variations of each fractal type, defined by the number of iterations applied, resulting in a stimuli set of 543. Eleven fractal types were used as demonstration and in practice trials, one type was used as a baseline trial that occurred 8 times across tasks, 72 types were randomly assigned to the Location Task, and 96 were randomly assigned to the Object Task (24 of these types were used as foil images during the Recognition phase). Fractal images used in the experiment are available here: https://github.com/zs-nemecz/TerKepEsz/tree/MRI_version/stimuli/fractals .

Experimental Design

We used two mnemonic discrimination tasks with either item or spatial similarity manipulation to test content-dependent interference reduction in the medial temporal lobe. The tasks were created in PsychoPy 2021.1.4 (Peirce et al., 2019). Each task consisted of an encoding and a recognition phase, divided into four scanner runs per task. During the whole task, a two-dimensional representation of the furnished interior of an art gallery was shown to participants, which contained an empty inner rectangle. We used such an art gallery framing to enhance the cover story of the task instructions – that participants are sorting and arranging artwork for an exhibition. Additionally, the gallery frame helped contextualize spatial locations in the Location Task.

Each trial consisted of a fractal appearing in the inner rectangle of the screen. Trial duration was 3s during the encoding phase, and 4s during the recognition phase. All trials were preceded by a fixation cross, which was presented at the center of the consecutive fractal's location for a jittered interval between 0.5 and 8 s.

After each encoding run and preceding the recognition run, participants had to solve a simple mathematical problem to reduce recency effects, which was followed by a short break (delay between last encoding trial and first recognition trial was around 2 minutes on average). Participants were aware of the memory manipulation already during encoding, and they were instructed before the recognition phase to pay

attention to small changes of fractals in the Object Task, and small changes of location in the Location Task.

Object Task: Encoding Phase

Participants made binary aesthetic judgements about each fractal, answering the following question: "Would you like to display this image in the exhibition of the art gallery?". This question served two purposes. First, we wanted to make sure participants attend to the features of each fractal. Second, although in principle passive viewing could have elicited our neural signals of interest, by requiring a response from participants, we could make sure that they pay attention throughout the task. The encoding phase consisted of 72 new (new fractal at a randomly assigned location), 48 lure (another version of the same fractal type, presented at the same location as the original), and 24 repeated (same fractal at the same location as the original) trials, in a pseudo-randomized order. We used twice as many lures than repeats to increase the power of detecting differences between lure bins, and small increases relative to repeats, assuming that repetition suppression is a robust effect that may be detectable with less trials than the sensitivity to lures.

Object Task: Recognition Phase

Participants had to make old/new memory judgements, corresponding to the following question: 'Have you seen exactly this image before?'. Twentyfour of the recognition trials were exactly repeated (same fractal at the same location as the original), 24 were lures (another version of the same fractal type, presented at the same location as the original), and 24 were foils (new fractal at a randomly assigned location).

Item Similarity Manipulation

Lure fractals in the Object Task were different versions of the same fractal type as the original fractal presented during encoding. The similarity between fractal versions was rated post-hoc by an independent sample of participants (n=30) on a scale from 0 ("Same") to 9 ("Very Different"). Details of the rating experiment and the distribution of fractal similarity values are included in the Supplementary Materials.

Location Task: Encoding Phase

The encoding phase of the Location Task was analogous to the encoding phase of the Object Task, but here lures were defined by their Euclidean distance to the first presentation of the fractal, not their within-item features. Participants made binary aesthetic judgments about the location of each fractal image. Specifically, participants had to decide whether they would like to display the presented image at the current location in the art gallery, which encouraged participants to pay attention to the location of each fractal. The encoding phase consisted of 72 new trials (new fractal at a randomly assigned location), 48 lure trials (repeated fractal at a location 200 to 350 pixels away from the original location), and 24 repeated trials (repeated fractal at the same location as the original), in a pseudo-randomized order.

Location Task: Recognition Phase

During the recognition phase, fractals were presented again in the inner rectangle of the screen, and participants had to make old/new memory judgements, corresponding to the following question: 'Have you seen this image exactly at this location?'. In the recognition phase of the Location Task, only fractals shown during the encoding phase were presented. Twentyfour of the recognition trials were exactly repeated relative to the first encoding presentation (same fractal, presented at the first, original location) and 48 were changed (same fractal, presented in a different location). Twenty-four of the changed trials were categorized as lures, and 24 were categorized as foils, based on the distance from the original, first encoding presentation of the trial (see the Spatial Similarity Manipulation section below).

Spatial Similarity Manipulation

During the encoding phase of the Location Task, lure trials consisted of repeated fractals presented 200 to 350 pixels away from their original location. The exact distance was randomly sampled from a uniform distribution. For the recognition phase, we originally grouped trials into repeated, lure and foil (i.e., very distant lure) conditions based on their Euclidean distance to the very first presentation of the fractal in the encoding phase. Twentyfour of the recognition trials were thus exactly repeated, twentyfour were lures separated by at least 200 and maximum 350 pixels, and 24 were

foils separated by at least 450 pixels. However, each trial's spatial similarity can also be calculated based on the Euclidean distance to the second presentation of the fractal during encoding, which also affected participants' "new" responses (Fig. 2). Distributions of lure and foil distances to the first and second presentation can be found in the supplementary materials (Suppl. Fig. 5).

Experimental Procedure

All participants completed both the Location and the Object Task. The order of the tasks was counterbalanced across participants. Participants were taken out of the scanner between the tasks for a longer break, and they were given the task-specific instructions immediately preceding the task. Before each task, participants were given 6 practice trials with feedback. Encoding and recognition phases were divided into two runs each, and participants completed them in an interleaved fashion, so that a recognition run followed each encoding run. For example, a participant starting with the Object Task had the following procedure: Object Task Instructions and Practice, Object Encoding 1, Object Recognition 1, Self-paced break in the scanner, Object Encoding 2, Object Recognition 2, Long break outside the scanner, Location Task Instructions and Practice, Location Encoding 1, Location Recognition 1, Self-paced break in the scanner, Location Encoding 2, Location Recognition 2.

Behavioral Data Analysis

We analyzed the ratio of "new" responses with a one-way repeated-measures ANOVA with the within factor condition (target, lure, foil) in Python 3.9.13 with statsmodels 0.13.2 (Seabold & Perktold, 2010). Follow-up paired sample t-tests were conducted with scipy 1.13.1 (Virtanen et al., 2020). Figures were created with matplotlib 3.9.2 (Hunter, 2007) and seaborn 0.13.0 (Waskom, 2021).

To further assess the effect of similarity per each trial, we used generalized binomial linear mixed effects modeling implemented in the R package lme4 1.1-31 (Bates et al., 2015). For each task, we built 3 models, predicting the probability of a "new" response per recognition trial. Assumption checks for the mixed effects models are described in the supplementary.

The first model (Model A) included the similarity between the first encoding trial and the recognition trial as a fixed effect predictor, and the participant-specific intercept as a random effects predictor. The second model (Model B) included the similarity between the second encoding trial and the recognition trial as a fixed effect predictor, and the participant-specific intercept as a random effects predictor. The third model (Model C) included the similarity between both the first and the second encoding trial and the recognition trial as fixed effect predictors, and the participant-specific intercept as a random effects predictor. Accordingly, for each task the three models were defined as below:

Model A: *RespNew* ~ *FirstSimilarity* + (1 | *Participant*),

Model B: *RespNew* ~ *SecondSimilarity* + (1 | *Participant*),

Model C: *RespNew* ~ *FirstSimilarity* * *SecondSimilarity* + (1 | *Participant*),

where *RespNew* is the probability of a "new" response, *FirstSimilarity* is the similarity between the first encoding trial and the recognition trial, and *SecondSimilarity* is the similarity between the second encoding trial and the recognition trial.

For the correlations between behavior and neural measures, we obtained the measures of individual sensitivity to similarity from modified versions of models A and B, which, in addition to the random intercepts, included random slopes. This type of model allows for the relationship between the explanatory variable (here: similarity) and the predicted variable (here: new response) to be different for each individual. Participant specific coefficients (individual slopes) were then extracted from the models.

MRI Data Acquisition

A Siemens Magnetom Prisma 3T MRI scanner (Siemens Healthcare, Erlangen, Germany) with the standard Siemens 32-channel head coil was used. Functional measurements were acquired with a conventional gradient-echo-EPI sequence using multiband-acceleration with factor 4 (80 slices, slice gap: 0.375 mm, slice ordering: interleaved, phase encoding direction: anterior to posterior, repetition time (TR) = 1840 ms, echo time (TE) = 30 ms, flip angle (FA) = 72°; field of view (FOV) = 204 mm, spatial resolution 1.5 × 1.5 × 1.5 mm). Fieldmaps for the functional runs were acquired each time

the participant was placed in the scanner, resulting in one fieldmap per task. We obtained sagittal T1-weighted images using a 3D MPRAGE sequence (TR = 2300 ms,TE = 3.03 ms, FA = 9°, FOV = 256 mm, spatial resolution 1 × 1 × 1 mm). An additional restricted FOV high-resolution proton-density (PD) weighted image of the medial temporal lobe area was acquired (TR = 6500 ms, TE = 16 ms, FA = 120°; spatial resolution 0.4 × 0.4 ×2 mm, FOV = 206 mm) to aid the delineation of the anatomical regions of interest.

Subject-level Region of Interest fMRI Data Analysis

Functional data preprocessing and analyses were done using FSL FEAT (Jenkinson et al., 2012; Woolrich et al., 2001, 2004, 2009). Functional runs were undistorted using fieldmaps and the T1 structural image. Then, each slice was spatially realigned to the middle slice within each volume with FSL MCFLIRT (Jenkinson et al., 2002), resulting in motion parameters that were used as regressors in further analysis for motion correction. As we strived to retain as much individual anatomical specificity as possible, functional runs were not transformed to the T1 or standard space for the region of interest analysis (see section "Registration of Anatomical Regions of Interest" below). In order to enable the analysis of multiple runs per subject in a single higher-level model, we used affine registration with 6 degrees of freedom to transform each run per participant to the same participant-specific functional space. To take advantage of the high spatial resolution functional scans, and considering the small size of hippocampal subfields, we applied minimal smoothing on the data with a 2-mm full-width at half-maximum isotropic Gaussian kernel. Finally, we applied a high-pass filter with a threshold of 90s on functional runs. The threshold of 90s was estimated by FSL Feat based on the trial timing.

For each participant, we performed two general linear model analyses using the data of the encoding phase. Regressors were defined by convolving the canonical hemodynamic response function with a boxcar function representing the onsets and duration of the events within each explanatory variable. In the first model, we defined four explanatory variables of interest: first presentation of later repeats, first presentation of later lures, repeats, and lures. In the second model, we collapsed all first presentation trials, and divided lure trials into high-similarity and low-similarity lure trials. This resulted in four explanatory variables of interest: repetition, high-similarity, low-similarity, and new (i.e., first presentation) trials. A single baseline trial was

repeated eight times across tasks. We included the first presentation of this trial among the first presentation of later repeat trials (and in the second model, among the merged first presentation trials), the second presentation among repeats, and the third to the eighth presentations were included in a separate explanatory variable in both models. We deemed the number of these multiple repetition trials too low to include them in further analysis, but exploratory results can be found in Supplementary Figure 2. In case of both GLM analyses, we included the six head motion parameters estimated in the realignment procedure and trial-wise reaction times (Mumford et al., 2024) as nuisance regressors. The resulting regressors were fitted to the observed functional time series of the encoding phase. Mean percent signal change values from all regions of interest were extracted from the individual participant space with FSL featquery and were analyzed with Python libraries scipy (Virtanen et al., 2020) and statsmodels (Seabold & Perktold, 2010), and R package lme4 (Bates et al., 2015).

Delineating Anatomical Regions of Interest in the MTL

Anatomical regions of interest (ROIs) were delineated on the high-resolution PD images with the software Automatic Segmentation of Hippocampal Subfields (ASHS, Yushkevich et al., 2015). We used the UPENN PMC Atlas (Yushkevich et al., 2015) for the segmentation of the perirhinal and parahippocampal cortices, and a custom atlas (Bender et al., 2018) for the delineation of subfields within the hippocampal body (cornu Ammonis 1-2: CA1, subiculum: SUB, cornu Ammonis 3 and dentate gyrus: CA3DG). Due to the less uniform structure of the hippocampal head and tail, no histologically validated segmentation protocols have yet been established for these regions (Bender et al., 2018; Wisse et al., 2017). Therefore, only the hippocampal body was segmented in this study. As in numerous previous high-resolution fMRI studies (Nash et al., 2021; Reagh & Yassa, 2014), the subfields CA3 and DG were combined into a single ROI (CA3DG). The quality of the segmentations was inspected by an experienced rater (A.K.), and errors were corrected following the recent guideline by Canada et al., 2023. Segmented regions were binarized and used as masks for extracting mean percent signal change values in the univariate and ROI-to-ROI connectivity analysis. An example segmentation is shown in Supplementary Figure 7.

Registration of Functional and High-Resolution Anatomical Images

We defined each participant's individual functional space as the mean volume of the first Object Encoding run. All other functional runs were registered to this volume with rigid body registration as implemented in FSL FLIRT (Jenkinson et al., 2002; Jenkinson & Smith, 2001) during the analysis of fMRI data. Anatomical masks were transformed into functional space with Advanced Normalization Tools (ANTs, Avants et al., 2009, 2011) using a three-step registration procedure. All input images were N4 bias-field corrected before registration. First, we registered the standard T1 anatomical image of each participant to the corresponding high-resolution partial field-of-view PD image with affine transformations, and obtained the transformation matrix *T1-to-PD*. Second, we registered the mean skull-stripped functional volume to the skull-stripped T1 anatomical image first using rigid transformation and then symmetric image normalization (SyN, Avants et al., 2008), and obtained the transformation matrix *meanFunc-to-T1* and warp image *meanFunc-to-T1*. For the meanFunc to T1 registration, we used a generous medial temporal lobe mask to optimize the registration outcome in this region. Exact parameters of the ANTs registration calls as well as registration examples can be found in the supplementary materials. Third, we transformed medial temporal ROIs derived from the PD space to functional space by applying the inverse of the *meanFunc-to-T1* matrix, the inverse of the *meanFunc-to-T1* warp, and finally the inverse of the *T1-to-PD* matrix.

Whole-brain Group-level fMRI analysis

We generated a group specific anatomical template with ANTs by registering individual T1 scans to a template space and then averaging them to form a whole-brain image representative of our sample. The average of all original T1 input images was used as the starting point for the iterative registration process. N4 bias field correction was applied on all input images before registration. One linear registration of input files was followed by four nonlinear SyN iterations. Each SyN registration was performed over four increasingly fine-grained resolutions ($100 \times 100 \times 70 \times 20$ iterations). The similarity metric was cross-correlation. Template update steps were set to 0.2 mm.

The fMRI data processing steps for the whole-brain analysis were identical to those of the subject-level region-of-interest analysis described above, with the

exception of registering functional runs to the individual T1 scans with BBR registration implemented in FSL (Greve & Fischl, 2009). Individual T1 scans were normalized to the group template with nonlinear registration to facilitate group-level analysis. Group-level contrast parameter estimate (COPE) images were transformed into MNI152 standard space, after coregistering the group T1 template image to the 1mm MNI152 template brain available in FLS. We obtained anatomical labels reported in the whole-brain group level results from the Harvard-Oxford Cortical Atlas (Desikan et al., 2006; Frazier et al., 2005; J. M. Goldstein et al., 2007; Makris et al., 2006).

Generalized Psychophysiological Interaction Analysis

The left and right angular gyrus, supramarginal gyrus, and middle frontal gyrus were used as anatomically defined seeds in the gPPI analyses. Cortical segmentations based on the Destrieux atlas (Destrieux et al., 2010; Fischl, 2004) were acquired for each participant using Freesurfer (Dale et al., 1999; Desikan et al., 2006; Fischl et al., 1999, 2002). Freesurfer segmentations were transformed into functional space, and ROI labels were extracted and binarized. Using the ROI masks, we derived the mean timeseries data from each functional run, and used these as physiological variables. One gPPI analysis was run per ROI. Besides the physiological variable, we included each condition from the encoding phase and its interaction with the physiological variable in the GLM as a regressor.

ROI-to-ROI Connectivity Analysis

We extracted the mean preprocessed timeseries data from each functional run using our medial temporal (left and right CA3DG, PHC, PRC) and frontoparietal (left and right angular gyrus, supramarginal gyrus, middle frontal gyrus) masks. Motion parameters were regressed out of all ROI timeseries data. Next, we correlated the timeseries data from each medial temporal region with all frontoparietal regions, and created one correlation matrix per functional run and subject. We applied Fisher's z transformation on the correlation coefficients, and then averaged matrices across runs of the same task, thus acquiring one correlation matrix per subject and task. We tested whether there is a significant connectivity between pairs of regions with one-sample t-tests. Connectivity differences between the Location and Object Encoding were tested with

paired sample t-tests. The relationship between connectivity and behavior was assessed with Spearman correlations, as we had no predictions on the linearity of the associations. Pearson correlations yielded the same pattern of results, but indicated stronger relationships between variables.

Data and code availability

Neuroimaging data: https://openneuro.org/datasets/ds005559/
Behavioral data:
https://osf.io/q9wks/?view_only=93849d7075374aad8dfce5b6c69e4e8a
Analysis code: https://github.com/zs-nemecz/miniTRK

Acknowledgments

We would like to thank Zoe Ngo, Myriam Sander, and Martin Dahl for helpful discussions about this project, and Eszter Somogyi and Dóra Bodócs for their assistance in data collection. This research was funded by the Hungarian National Research, Development and Innovation Office (FK128648). A.K. was additionally supported by a Max Planck Partner Group from the Max Planck Society, by a Bolyai János Research Scholarship of the Hungarian Academy of Sciences, and by the HUN-REN (grant 0708-21 515 AT). Parts of the work in this manuscript were conducted while Z.N. was a guest scientist at the Center for Lifespan Psychology, Max Planck Institute for Human Development, Berlin. Z.N. was supported by a One-Year Grant for Doctoral Candidates from the German Academic Exchange Service, and by the ÚNKP-22-3 New National Excellence Program of the Ministry for Culture and Innovation from the source of the National Research, Development and Innovation Fund. We are grateful for the services provided by the HUN-REN Cloud (Héder et al., 2022; https://science-cloud.hu/), where parts of the presented data were analyzed.

References

Aimone, J. B., Deng, W., & Gage, F. H. (2011). Resolving New Memories: A Critical Look at the Dentate Gyrus, Adult Neurogenesis, and Pattern Separation. *Neuron*, 70(4), 589–596. https://doi.org/10.1016/j.neuron.2011.05.010https://doi.org/10.1002/hbm.22627

Amer, T., & Davachi, L. (2023). Extra-hippocampal contributions to pattern separation. *eLife*, 12, e82250. https://doi.org/10.7554/eLife.82250

Anderson, M. C., & Hulbert, J. C. (2021). Active Forgetting: Adaptation of Memory by Prefrontal Control. *Annual Review of Psychology*, 72(Volume 72, 2021), 1–36. https://doi.org/10.1146/annurev-psych-072720-094140

Anderson, M. C., Ochsner, K. N., Kuhl, B., Cooper, J., Robertson, E., Gabrieli, S. W., Glover, G. H., & Gabrieli, J. D. E. (2004). Neural Systems Underlying the Suppression of Unwanted Memories. *Science*, 303(5655), 232–235. https://doi.org/10.1126/science.1089504

Asp, I. E., Störmer, V. S., & Brady, T. F. (2021). Greater Visual Working Memory Capacity for Visually Matched Stimuli When They Are Perceived as Meaningful. *Journal of Cognitive Neuroscience*, 33(5), 902–918. https://doi.org/10.1162/jocn_a_01693

Avants, B. B., Epstein, C. L., Grossman, M., & Gee, J. C. (2008). Symmetric diffeomorphic image registration with cross-correlation: Evaluating automated labeling of elderly and neurodegenerative brain. *Medical Image Analysis*, 12(1), 26–41. https://doi.org/10.1016/j.media.2007.06.004

Avants, B. B., Tustison, N. J., Song, G., Cook, P. A., Klein, A., & Gee, J. C. (2011). A reproducible evaluation of ANTs similarity metric performance in brain image registration. *NeuroImage*, 54(3), 2033–2044.

https://doi.org/10.1016/j.neuroimage.2010.09.025

Avants, B. B., Tustison, N., Song, G., & others. (2009). Advanced normalization tools (ANTS). *Insight j*, *2*(365), 1–35.

Azab, M., Stark, S. M., & Stark, C. E. L. (2014). Contributions of human hippocampal subfields to spatial and temporal pattern separation. *Hippocampus*, *24*(3), 293–302. https://doi.org/10.1002/hipo.22223

Baker, S., Vieweg, P., Gao, F., Gilboa, A., Wolbers, T., Black, S. E., & Rosenbaum, R. S. (2016). The Human Dentate Gyrus Plays a Necessary Role in Discriminating New Memories. *Current Biology*, *26*(19), 2629–2634. https://doi.org/10.1016/j.cub.2016.07.081

Bakker, A., Kirwan, C. B., Miller, M., & Stark, C. E. L. (2008). Pattern Separation in the Human Hippocampal CA3 and Dentate Gyrus. *Science*, *319*(5870), 1640–1642. https://doi.org/10.1126/science.1152882

Barense, M. D., Bussey, T. J., Lee, A. C. H., Rogers, T. T., Davies, R. R., Saksida, L. M., Murray, E. A., & Graham, K. S. (2005). Functional Specialization in the Human Medial Temporal Lobe. *Journal of Neuroscience*, *25*(44), 10239–10246. https://doi.org/10.1523/JNEUROSCI.2704-05.2005

Barense, M. D., Henson, R. N. A., & Graham, K. S. (2011). Perception and Conception: Temporal Lobe Activity during Complex Discriminations of Familiar and Novel Faces and Objects. *Journal of Cognitive Neuroscience*, *23*(10), 3052–3067. https://doi.org/10.1162/jocn_a_00010

Barense, M. D., Henson, R. N. A., Lee, A. C. H., & Graham, K. S. (2010). Medial temporal lobe activity during complex discrimination of faces, objects, and scenes: Effects of viewpoint. *Hippocampus*, *20*(3), 389–401. https://doi.org/10.1002/hipo.20641

Bartlett, F. C. (1995). *Remembering: A study in experimental and social psychology*.

Cambridge university press.

Bates, D., Mächler, M., Bolker, B., & Walker, S. (2015). Fitting Linear Mixed-Effects Models Using lme4. *Journal of Statistical Software*, 67(1), 1–48. https://doi.org/10.18637/jss.v067.i01

Bencze, D., Marián, M., Szőllősi, Á., Pajkossy, P., Nemecz, Z., Keresztes, A., Hermann, P., Vidnyánszky, Z., & Racsmány, M. (2024). Contribution of the lateral occipital and parahippocampal cortices to pattern separation of objects and contexts. *Cerebral Cortex*, 34(7), bhae295. https://doi.org/10.1093/cercor/bhae295

Bender, A. R., Keresztes, A., Bodammer, N. C., Shing, Y. L., Werkle-Bergner, M., Daugherty, A. M., Yu, Q., Kühn, S., Lindenberger, U., & Raz, N. (2018). Optimization and validation of automated hippocampal subfield segmentation across the lifespan. *Human Brain Mapping*, 39(2), 916–931. https://doi.org/10.1002/hbm.23891

Benjamini, Y., & Hochberg, Y. (1995). Controlling the False Discovery Rate: A Practical and Powerful Approach to Multiple Testing. *Journal of the Royal Statistical Society: Series B (Methodological)*, 57(1), 289–300. https://doi.org/10.1111/j.2517-6161.1995.tb02031.x

Berron, D., Neumann, K., Maass, A., Schütze, H., Fliessbach, K., Kiven, V., Jessen, F., Sauvage, M., Kumaran, D., & Düzel, E. (2018). Age-related functional changes in domain-specific medial temporal lobe pathways. *Neurobiology of Aging*, 65, 86–97. https://doi.org/10.1016/j.neurobiolaging.2017.12.030

Berron, D., Schütze, H., Maass, A., Cardenas-Blanco, A., Kuijf, H. J., Kumaran, D., & Düzel, E. (2016). Strong Evidence for Pattern Separation in Human Dentate Gyrus. *Journal of Neuroscience*, 36(29), 7569–7579. https://doi.org/10.1523/JNEUROSCI.0518-16.2016

Brady, T. F., Alvarez, G. A., & Störmer, V. S. (2019). The Role of Meaning in Visual Memory: Face-Selective Brain Activity Predicts Memory for Ambiguous Face Stimuli. *Journal of Neuroscience*, 39(6), 1100–1108. https://doi.org/10.1523/JNEUROSCI.1693-18.2018

Brickman, A. M., Khan, U. A., Provenzano, F. A., Yeung, L.-K., Suzuki, W., Schroeter, H., Wall, M., Sloan, R. P., & Small, S. A. (2014). Enhancing dentate gyrus function with dietary flavanols improves cognition in older adults. *Nature Neuroscience*, 17(12), 1798–1803. https://doi.org/10.1038/nn.3850

Broadbent, N. J., Squire, L. R., & Clark, R. E. (2004). Spatial memory, recognition memory, and the hippocampus. *Proceedings of the National Academy of Sciences*, 101(40), 14515–14520. https://doi.org/10.1073/pnas.0406344101

Burke, S. N., Gaynor, L. S., Barnes, C. A., Bauer, R. M., Bizon, J. L., Roberson, E. D., & Ryan, L. (2018). Shared Functions of Perirhinal and Parahippocampal Cortices: Implications for Cognitive Aging. *Trends in Neurosciences*, 41(6), 349–359. https://doi.org/10.1016/j.tins.2018.03.001

Burke, S. N., Maurer, A. P., Nematollahi, S., Uprety, A., Wallace, J. L., & Barnes, C. A. (2014). Advanced Age Dissociates Dual Functions of the Perirhinal Cortex. *Journal of Neuroscience*, 34(2), 467–480. https://doi.org/10.1523/JNEUROSCI.2875-13.2014

Burwell, R. D., & Amaral, D. G. (1998a). Cortical afferents of the perirhinal, postrhinal, and entorhinal cortices of the rat. *Journal of Comparative Neurology*, 398(2), 179–205. https://doi.org/10.1002/(SICI)1096-9861(19980824)398:2<179::AID-CNE3>3.0.CO;2-Y

Burwell, R. D., & Amaral, D. G. (1998b). Perirhinal and postrhinal cortices of the rat: Interconnectivity and connections with the entorhinal cortex. *Journal of Comparative Neurology*, 391(3), 293–321.

https://doi.org/10.1002/(SICI)1096-9861(19980216)391:3<293::AID-CNE2>3.0.CO;2-X

Bussey, T. J., Saksida, L. M., & Murray, E. A. (2002). Perirhinal cortex resolves feature ambiguity in complex visual discriminations. *European Journal of Neuroscience*, *15*(2), 365–374. https://doi.org/10.1046/j.0953-816x.2001.01851.x

Canada, K. L., Mazloum-Farzaghi, N., Rådman, G., Adams, J. N., Bakker, A., Baumeister, H., Berron, D., Bocchetta, M., Carr, V., Dalton, M. A., Flores, R. de, Keresztes, A., Joie, R. L., Mueller, S. G., Raz, N., Santini, T., Shaw, T., Stark, C. E. L., Tran, T. T., … Group, the H. S. (2023). *A (Sub)field Guide to Quality Control in Hippocampal Subfield Segmentation on High-resolution T2-weighted MRI* (p. 2023.11.29.568895). bioRxiv. https://doi.org/10.1101/2023.11.29.568895

Cayco-Gajic, N. A., & Silver, R. A. (2019). Re-evaluating Circuit Mechanisms Underlying Pattern Separation. *Neuron*, *101*(4), 584–602. https://doi.org/10.1016/j.neuron.2019.01.044

Chanales, A. J. H., Oza, A., Favila, S. E., & Kuhl, B. A. (2017). Overlap among Spatial Memories Triggers Repulsion of Hippocampal Representations. *Current Biology*, *27*(15), 2307-2317.e5. https://doi.org/10.1016/j.cub.2017.06.057

Chanales, A. J. H., Tremblay-McGaw, A. G., Drascher, M. L., & Kuhl, B. A. (2021). Adaptive Repulsion of Long-Term Memory Representations Is Triggered by Event Similarity. *Psychological Science*, *32*(5), 705–720. https://doi.org/10.1177/0956797620972490

Connor, C. E., & Knierim, J. J. (2017). Integration of objects and space in perception and memory. *Nature Neuroscience*, *20*(11), 1493–1503. https://doi.org/10.1038/nn.4657

Cowell, R. A., Barense, M. D., & Sadil, P. S. (2019). A Roadmap for Understanding Memory: Decomposing Cognitive Processes into Operations and Representations. *eNeuro*,

6(4). https://doi.org/10.1523/ENEURO.0122-19.2019

Dale, A., Fischl, B., & Sereno, M. I. (1999). Cortical Surface-Based Analysis: I. Segmentation and Surface Reconstruction. *NeuroImage*, *9*(2), 179–194.

Depue, B. E., Orr, J. M., Smolker, H. R., Naaz, F., & Banich, M. T. (2016). The Organization of Right Prefrontal Networks Reveals Common Mechanisms of Inhibitory Regulation Across Cognitive, Emotional, and Motor Processes. *Cerebral Cortex*, *26*(4), 1634–1646. https://doi.org/10.1093/cercor/bhu324

Desikan, R. S., Ségonne, F., Fischl, B., Quinn, B. T., Dickerson, B. C., Blacker, D., Buckner, R. L., Dale, A. M., Maguire, R. P., Hyman, B. T., Albert, M. S., & Killiany, R. J. (2006). An automated labeling system for subdividing the human cerebral cortex on MRI scans into gyral based regions of interest. *NeuroImage*, *31*(3), 968–980. https://doi.org/10.1016/j.neuroimage.2006.01.021

Destrieux, C., Fischl, B., Dale, A., & Halgren, E. (2010). Automatic parcellation of human cortical gyri and sulci using standard anatomical nomenclature. *NeuroImage*, *53*(1), 1–15. https://doi.org/10.1016/j.neuroimage.2010.06.010

Deuker, L., Doeller, C., Fell, J., & Axmacher, N. (2014). Human neuroimaging studies on the hippocampal CA3 region – integrating evidence for pattern separation and completion. *Frontiers in Cellular Neuroscience*, *8*. https://doi.org/10.3389/fncel.2014.00064

Di, X., & Biswal, B. B. (2017). Psychophysiological Interactions in a Visual Checkerboard Task: Reproducibility, Reliability, and the Effects of Deconvolution. *Frontiers in Neuroscience*, *11*. https://doi.org/10.3389/fnins.2017.00573

Di, X., Zhang, Z., & Biswal, B. B. (2021). Understanding psychophysiological interaction and its relations to beta series correlation. *Brain Imaging and Behavior*, *15*(2), 958–973. https://doi.org/10.1007/s11682-020-00304-8

Dimsdale-Zucker, H. R., Ritchey, M., Ekstrom, A. D., Yonelinas, A. P., & Ranganath, C. (2018). CA1 and CA3 differentially support spontaneous retrieval of episodic contexts within human hippocampal subfields. *Nature Communications*, 9(1), Article 1. https://doi.org/10.1038/s41467-017-02752-1

Dixon, M. L., De La Vega, A., Mills, C., Andrews-Hanna, J., Spreng, R. N., Cole, M. W., & Christoff, K. (2018). Heterogeneity within the frontoparietal control network and its relationship to the default and dorsal attention networks. *Proceedings of the National Academy of Sciences*, 115(7), E1598–E1607. https://doi.org/10.1073/pnas.1715766115

Duff, M. C., Warren, D. E., Gupta, R., Vidal, J. P. B., Tranel, D., & Cohen, N. J. (2012). Teasing apart tangrams: Testing hippocampal pattern separation with a collaborative referencing paradigm. *Hippocampus*, 22(5), 1087–1091. https://doi.org/10.1002/hipo.20967

Eacott, M. J., & Gaffan, E. A. (2005). The Roles of Perirhinal Cortex, Postrhinal Cortex, and the Fornix in Memory for Objects, Contexts, and Events in the Rat. *The Quarterly Journal of Experimental Psychology Section B*, 58(3–4b), 202–217. https://doi.org/10.1080/02724990444000203

Favila, S. E., Chanales, A. J. H., & Kuhl, B. A. (2016). Experience-dependent hippocampal pattern differentiation prevents interference during subsequent learning. *Nature Communications*, 7(1), 11066. https://doi.org/10.1038/ncomms11066

Fischl, B. (2004). Automatically Parcellating the Human Cerebral Cortex. *Cerebral Cortex*, 14(1), 11–22. https://doi.org/10.1093/cercor/bhg087

Fischl, B., Salat, D. H., Busa, E., Albert, M., Dieterich, M., Haselgrove, C., van der Kouwe, A., Killiany, R., Kennedy, D., Klaveness, S., Montillo, A., Makris, N., Rosen, B., & Dale, A. M. (2002). Whole brain segmentation: Automated labeling of

neuroanatomical structures in the human brain. *Neuron*, 33, 341–355.

Fischl, B., Sereno, M. I., & Dale, A. (1999). Cortical Surface-Based Analysis: II: Inflation, Flattening, and a Surface-Based Coordinate System. *NeuroImage*, 9(2), 195–207.

Frazier, J. A., Chiu, S., Breeze, J. L., Makris, N., Lange, N., Kennedy, D. N., Herbert, M. R., Bent, E. K., Koneru, V. K., Dieterich, M. E., Hodge, S. M., Rauch, S. L., Grant, P. E., Cohen, B. M., Seidman, L. J., Caviness, V. S., & Biederman, J. (2005). Structural Brain Magnetic Resonance Imaging of Limbic and Thalamic Volumes in Pediatric Bipolar Disorder. *American Journal of Psychiatry*, 162(7), 1256–1265. https://doi.org/10.1176/appi.ajp.162.7.1256

Friston, K. J., Buechel, C., Fink, G. R., Morris, J., Rolls, E., & Dolan, R. J. (1997). Psychophysiological and Modulatory Interactions in Neuroimaging. *NeuroImage*, 6(3), 218–229. https://doi.org/10.1006/nimg.1997.0291

Gaffan, E. A., Healey, A. N., & Eacott, M. J. (2004). Objects and Positions in Visual Scenes: Effects of Perirhinal and Postrhinal Cortex Lesions in the Rat. *Behavioral Neuroscience*, 118(5), 992–1010. https://doi.org/10.1037/0735-7044.118.5.992

Gilbert, P. E., Kesner, R. P., & Lee, I. (2001). Dissociating hippocampal subregions: A double dissociation between dentate gyrus and CA1. *Hippocampus*, 11(6), 626–636. https://doi.org/10.1002/hipo.1077

Goldstein, A. G., & Chance, J. E. (1971). Visual recognition memory for complex configurations. *Perception & Psychophysics*, 9(2), 237–241. https://doi.org/10.3758/BF03212641

Goldstein, J. M., Seidman, L. J., Makris, N., Ahern, T., O'Brien, L. M., Caviness, V. S., Kennedy, D. N., Faraone, S. V., & Tsuang, M. T. (2007). Hypothalamic Abnormalities in Schizophrenia: Sex Effects and Genetic Vulnerability. *Biological Psychiatry*, 61(8), 935–945. https://doi.org/10.1016/j.biopsych.2006.06.027

Goodrich-Hunsaker, N. J., Hunsaker, M. R., & Kesner, R. P. (2008). The interactions and dissociations of the dorsal hippocampus subregions: How the dentate gyrus, CA3, and CA1 process spatial information. *Behavioral Neuroscience*, 122(1), 16–26. https://doi.org/10.1037/0735-7044.122.1.16

GoodSmith, D., Lee, H., Neunuebel, J. P., Song, H., & Knierim, J. J. (2019). Dentate Gyrus Mossy Cells Share a Role in Pattern Separation with Dentate Granule Cells and Proximal CA3 Pyramidal Cells. *Journal of Neuroscience*, 39(48), 9570–9584. https://doi.org/10.1523/JNEUROSCI.0940-19.2019

Greve, D. N., & Fischl, B. (2009). Accurate and robust brain image alignment using boundary-based registration. *NeuroImage*, 48(1), 63–72. https://doi.org/10.1016/j.neuroimage.2009.06.060

Grill-Spector, K., Henson, R., & Martin, A. (2006). Repetition and the brain: Neural models of stimulus-specific effects. *Trends in Cognitive Sciences*, 10(1), 14–23. https://doi.org/10.1016/j.tics.2005.11.006

Hartley, T., Lever, C., Burgess, N., & O'Keefe, J. (2014). Space in the brain: How the hippocampal formation supports spatial cognition. *Philosophical Transactions of the Royal Society B: Biological Sciences*, 369(1635), 20120510. https://doi.org/10.1098/rstb.2012.0510

Héder, M., Rigó, E., Medgyesi, D., Lovas, R., Tenczer, S., Török, F., Farkas, A., Emődi, M., Kadlecsik, J., Mező, G., Pintér, Á., & Kacsuk, P. (2022). The Past, Present and Future of the ELKH Cloud. *Információs Társadalom*, 22(2), 128. https://doi.org/10.22503/inftars.XXII.2022.2.8

Hunsaker, M. R., & Kesner, R. P. (2013). The operation of pattern separation and pattern completion processes associated with different attributes or domains of memory. *Neuroscience & Biobehavioral Reviews*, 37(1), 36–58.

https://doi.org/10.1016/j.neubiorev.2012.09.014

Hunsaker, M. R., Rosenberg, J. S., & Kesner, R. P. (2008). The role of the dentate gyrus, CA3a,b, and CA3c for detecting spatial and environmental novelty. *Hippocampus*, *18*(10), 1064–1073. https://doi.org/10.1002/hipo.20464

Hunter, J. D. (2007). Matplotlib: A 2D graphics environment. *Computing in Science & Engineering*, *9*(3), 90–95. https://doi.org/10.1109/MCSE.2007.55

Jenkinson, M., Bannister, P., Brady, M., & Smith, S. (2002). Improved Optimization for the Robust and Accurate Linear Registration and Motion Correction of Brain Images. *NeuroImage*, *17*(2), 825–841. https://doi.org/10.1006/nimg.2002.1132

Jenkinson, M., Beckmann, C. F., Behrens, T. E. J., Woolrich, M. W., & Smith, S. M. (2012). FSL. *NeuroImage*, *62*(2), 782–790. https://doi.org/10.1016/j.neuroimage.2011.09.015

Jenkinson, M., & Smith, S. (2001). A global optimisation method for robust affine registration of brain images. *Medical Image Analysis*, *5*(2), 143–156. https://doi.org/10.1016/S1361-8415(01)00036-6

Johnston, S. T., Shtrahman, M., Parylak, S., Gonçalves, J. T., & Gage, F. H. (2016). Paradox of pattern separation and adult neurogenesis: A dual role for new neurons balancing memory resolution and robustness. *Neurobiology of Learning and Memory*, *129*, 60–68. https://doi.org/10.1016/j.nlm.2015.10.013

Kirwan, C. B., & Stark, C. E. L. (2007). Overcoming interference: An fMRI investigation of pattern separation in the medial temporal lobe. *Learning & Memory*, *14*(9), 625–633. https://doi.org/10.1101/lm.663507

Klippenstein, J. L., Stark, S. M., Stark, C. E. L., & Bennett, I. J. (2020). Neural substrates of mnemonic discrimination: A whole-brain fMRI investigation. *Brain and Behavior*, *10*(3), e01560. https://doi.org/10.1002/brb3.1560

Knierim, J. J., & Neunuebel, J. P. (2016). Tracking the flow of hippocampal computation: Pattern separation, pattern completion, and attractor dynamics. *Neurobiology of Learning and Memory*, 129, 38–49. https://doi.org/10.1016/j.nlm.2015.10.008

Knierim, J. J., Neunuebel, J. P., & Deshmukh, S. S. (2014). Functional correlates of the lateral and medial entorhinal cortex: Objects, path integration and local–global reference frames. *Philosophical Transactions of the Royal Society B: Biological Sciences*, 369(1635), 20130369. https://doi.org/10.1098/rstb.2013.0369

Kumaran, D., Hassabis, D., & McClelland, J. L. (2016). What Learning Systems do Intelligent Agents Need? Complementary Learning Systems Theory Updated. *Trends in Cognitive Sciences*, 20(7), 512–534. https://doi.org/10.1016/j.tics.2016.05.004

Kyle, C. T., Stokes, J. D., Lieberman, J. S., Hassan, A. S., & Ekstrom, A. D. (2015). Successful retrieval of competing spatial environments in humans involves hippocampal pattern separation mechanisms. *eLife*, 4, e10499. https://doi.org/10.7554/eLife.10499

Lawrence, A. V., Cardoza, J., & Ryan, L. (2020). Medial temporal lobe regions mediate complex visual discriminations for both objects and scenes: A process-based view. *Hippocampus*, hipo.23203. https://doi.org/10.1002/hipo.23203

Leal, S. L., & Yassa, M. A. (2018). Integrating new findings and examining clinical applications of pattern separation. *Nature Neuroscience*, 21(2), Article 2. https://doi.org/10.1038/s41593-017-0065-1

Lee, H., GoodSmith, D., & Knierim, J. J. (2020). Parallel processing streams in the hippocampus. *Current Opinion in Neurobiology*, 64, 127–134. https://doi.org/10.1016/j.conb.2020.03.004

Leutgeb, J. K., Leutgeb, S., Moser, M.-B., & Moser, E. I. (2007). Pattern Separation in the

Dentate Gyrus and CA3 of the Hippocampus. *Science*, 315(5814), 961–966. https://doi.org/10.1126/science.1135801

Liu, K. Y., Gould, R. L., Coulson, M. C., Ward, E. V., & Howard, R. J. (2016). Tests of pattern separation and pattern completion in humans—A systematic review. *Hippocampus*, 26(6), 705–717. https://doi.org/10.1002/hipo.22561

Loiotile, R. E., & Courtney, S. M. (2015). A signal detection theory analysis of behavioral pattern separation paradigms. *Learning & Memory*, 22(8), 364–369. https://doi.org/10.1101/lm.038141.115

Maass, A., Berron, D., Libby, L. A., Ranganath, C., & Düzel, E. (2015). Functional subregions of the human entorhinal cortex. *eLife*, 4, e06426. https://doi.org/10.7554/eLife.06426

Makris, N., Goldstein, J. M., Kennedy, D., Hodge, S. M., Caviness, V. S., Faraone, S. V., Tsuang, M. T., & Seidman, L. J. (2006). Decreased volume of left and total anterior insular lobule in schizophrenia. *Schizophrenia Research*, 83(2), 155–171. https://doi.org/10.1016/j.schres.2005.11.020

Marr, D. (1971). Simple memory: A theory for archicortex. *Philosophical Transactions of the Royal Society of London. Series B, Biological Sciences*, 262(841), 23–81. https://doi.org/10.1098/rstb.1971.0078

Martin, C. B., & Barense, M. D. (2023). Perception and Memory in the Ventral Visual Stream and Medial Temporal Lobe. *Annual Review of Vision Science*, 9(1), 409–434. https://doi.org/10.1146/annurev-vision-120222-014200

McClelland, J. L., McNaughton, B. L., & O'Reilly, R. C. (1995). Why there are complementary learning systems in the hippocampus and neocortex: Insights from the successes and failures of connectionist models of learning and memory. *Psychological Review*, 102(3), 419–457.

https://doi.org/10.1037/0033-295X.102.3.419

McCloskey, M., & Cohen, N. J. (1989). Catastrophic Interference in Connectionist Networks: The Sequential Learning Problem. In G. H. Bower (Ed.), *Psychology of Learning and Motivation* (Vol. 24, pp. 109–165). Academic Press. https://doi.org/10.1016/S0079-7421(08)60536-8

McHugh, T. J., Jones, M. W., Quinn, J. J., Balthasar, N., Coppari, R., Elmquist, J. K., Lowell, B. B., Fanselow, M. S., Wilson, M. A., & Tonegawa, S. (2007). Dentate Gyrus NMDA Receptors Mediate Rapid Pattern Separation in the Hippocampal Network. *Science*, 317(5834), 94–99. https://doi.org/10.1126/science.1140263

McLaren, D. G., Ries, M. L., Xu, G., & Johnson, S. C. (2012). A Generalized Form of Context-Dependent Psychophysiological Interactions (gPPI): A Comparison to Standard Approaches. *Neuroimage*, 61(4), 1277–1286. https://doi.org/10.1016/j.neuroimage.2012.03.068

Mitchnick, K. A., Ahmad, Z., Mitchnick, S. D., Ryan, J. D., Rosenbaum, R. S., & Freud, E. (2022). Damage to the human dentate gyrus impairs the perceptual discrimination of complex, novel objects. *Neuropsychologia*, 172, 108238. https://doi.org/10.1016/j.neuropsychologia.2022.108238

Mitchnick, K. A., Marlatte, H., Belchev, Z., Gao, F., & Rosenbaum, R. S. (2024). Differential contributions of the hippocampal dentate gyrus and CA1 subfield to mnemonic discrimination. *Hippocampus*, 34(6), 278–283. https://doi.org/10.1002/hipo.23604

Molitor, R. J., Ko, P. C., Hussey, E. P., & Ally, B. A. (2014). Memory-related eye movements challenge behavioral measures of pattern completion and pattern separation. *Hippocampus*, 24(6), 666–672. https://doi.org/10.1002/hipo.22256

Motley, S. E., & Kirwan, C. B. (2012). A Parametric Investigation of Pattern Separation

Processes in the Medial Temporal Lobe. *Journal of Neuroscience*, 32(38), 13076–13084. https://doi.org/10.1523/JNEUROSCI.5920-11.2012

Mumford, J. A., Bissett, P. G., Jones, H. M., Shim, S., Rios, J. A. H., & Poldrack, R. A. (2024). The response time paradox in functional magnetic resonance imaging analyses. *Nature Human Behaviour*, 8(2), 349–360. https://doi.org/10.1038/s41562-023-01760-0

Nash, M. I., Hodges, C. B., Muncy, N. M., & Kirwan, C. B. (2021). Pattern separation beyond the hippocampus: A high-resolution whole-brain investigation of mnemonic discrimination in healthy adults. *Hippocampus*, 31(4), 408–421. https://doi.org/10.1002/hipo.23299

Neunuebel, J. P., & Knierim, J. J. (2014). CA3 retrieves coherent representations from degraded input: Direct evidence for CA3 pattern completion and dentate gyrus pattern separation. *Neuron*, 81(2), 416–427. https://doi.org/10.1016/j.neuron.2013.11.017

Nilssen, E. S., Doan, T. P., Nigro, M. J., Ohara, S., & Witter, M. P. (2019). Neurons and networks in the entorhinal cortex: A reappraisal of the lateral and medial entorhinal subdivisions mediating parallel cortical pathways. *Hippocampus*, 29(12), 1238–1254. https://doi.org/10.1002/hipo.23145

O'Reilly, J. X., Woolrich, M. W., Behrens, T. E. J., Smith, S. M., & Johansen-Berg, H. (2012). Tools of the trade: Psychophysiological interactions and functional connectivity. *Social Cognitive and Affective Neuroscience*, 7(5), 604–609. https://doi.org/10.1093/scan/nss055

O'Reilly, R. C., Bhattacharyya, R., Howard, M. D., & Ketz, N. (2014). Complementary Learning Systems. *Cognitive Science*, 38(6), 1229–1248. https://doi.org/10.1111/j.1551-6709.2011.01214.x

O'Reilly, R. C., & McClelland, J. L. (1994). Hippocampal conjunctive encoding, storage, and recall: Avoiding a trade-off. *Hippocampus*, 4(6), 661–682. https://doi.org/10.1002/hipo.450040605

Paleja, M., Girard, T. A., Herdman, K. A., & Christensen, B. K. (2014). Two distinct neural networks functionally connected to the human hippocampus during pattern separation tasks. *Brain and Cognition*, 92, 101–111. https://doi.org/10.1016/j.bandc.2014.10.009

Peirce, J., Gray, J. R., Simpson, S., MacAskill, M., Höchenberger, R., Sogo, H., Kastman, E., & Lindeløv, J. K. (2019). PsychoPy2: Experiments in behavior made easy. *Behavior Research Methods*, 51(1), 195–203. https://doi.org/10.3758/s13428-018-01193-y

Quiroga, R. Q. (2020). No Pattern Separation in the Human Hippocampus. *Trends in Cognitive Sciences*, 24(12), 994–1007. https://doi.org/10.1016/j.tics.2020.09.012

Reagh, Z. M., & Yassa, M. A. (2014). Object and spatial mnemonic interference differentially engage lateral and medial entorhinal cortex in humans. *Proceedings of the National Academy of Sciences*, 111(40), E4264–E4273. https://doi.org/10.1073/pnas.1411250111

Rolls, E. T. (2013). The mechanisms for pattern completion and pattern separation in the hippocampus. *Frontiers in Systems Neuroscience*, 7. https://doi.org/10.3389/fnsys.2013.00074

Rolls, E. T. (2024). Two what, two where, visual cortical streams in humans. *Neuroscience & Biobehavioral Reviews*, 160, 105650. https://doi.org/10.1016/j.neubiorev.2024.105650

Sakon, J. J., & Suzuki, W. A. (2019). A neural signature of pattern separation in the monkey hippocampus. *Proceedings of the National Academy of Sciences*, 116(19), 9634–9643. https://doi.org/10.1073/pnas.1900804116

Seabold, S., & Perktold, J. (2010). statsmodels: Econometric and statistical modeling with python. *9th Python in Science Conference*.

Staresina, B. P., Duncan, K. D., & Davachi, L. (2011). Perirhinal and Parahippocampal Cortices Differentially Contribute to Later Recollection of Object- and Scene-Related Event Details. *Journal of Neuroscience*, 31(24), 8739–8747. https://doi.org/10.1523/JNEUROSCI.4978-10.2011

Stark, S. M., Kirwan, C. B., & Stark, C. E. L. (2019). Mnemonic Similarity Task: A Tool for Assessing Hippocampal Integrity. *Trends in Cognitive Sciences*, 23(11), 938–951. https://doi.org/10.1016/j.tics.2019.08.003

Stark, S. M., Stevenson, R., Wu, C., Rutledge, S., & Stark, C. E. L. (2015). Stability of age-related deficits in the mnemonic similarity task across task variations. *Behavioral Neuroscience*, 129(3), 257–268. https://doi.org/10.1037/bne0000055

Stark, S. M., Yassa, M. A., Lacy, J. W., & Stark, C. E. L. (2013). A task to assess behavioral pattern separation (BPS) in humans: Data from healthy aging and mild cognitive impairment. *Neuropsychologia*, 51(12), 2442–2449. https://doi.org/10.1016/j.neuropsychologia.2012.12.014

Uddin, L. Q., Yeo, B. T. T., & Spreng, R. N. (2019). Towards a universal taxonomy of macro-scale functional human brain networks. *Brain Topography*, 32(6), 926. https://doi.org/10.1007/s10548-019-00744-6

Virtanen, P., Gommers, R., Oliphant, T. E., Haberland, M., Reddy, T., Cournapeau, D., Burovski, E., Peterson, P., Weckesser, W., Bright, J., van der Walt, S. J., Brett, M., Wilson, J., Millman, K. J., Mayorov, N., Nelson, A. R. J., Jones, E., Kern, R., Larson, E., … SciPy 1.0 Contributors. (2020). SciPy 1.0: Fundamental Algorithms for Scientific Computing in Python. *Nature Methods*, 17, 261–272. https://doi.org/10.1038/s41592-019-0686-2

Wanjia, G., Favila, S. E., Kim, G., Molitor, R. J., & Kuhl, B. A. (2021). Abrupt hippocampal remapping signals resolution of memory interference. *Nature Communications*, *12*(1), 4816. https://doi.org/10.1038/s41467-021-25126-0

Waskom, M. L. (2021). seaborn: Statistical data visualization. *Journal of Open Source Software*, *6*(60), 3021. https://doi.org/10.21105/joss.03021

Weeden, C. S. S., Hu, N. J., Ho, L. U. N., & Kesner, R. P. (2014). The role of the ventral dentate gyrus in olfactory pattern separation. *Hippocampus*, *24*(5), 553–559. https://doi.org/10.1002/hipo.22248

Williams, L., Störmer, V. S., Brady, T., & Brady, T. (2023). *The working memory advantage for meaningful stimuli persists under high levels of proactive interference*. https://osf.io/e5fkz/download

Wimber, M., Alink, A., Charest, I., Kriegeskorte, N., & Anderson, M. C. (2015). Retrieval induces adaptive forgetting of competing memories via cortical pattern suppression. *Nature Neuroscience*, *18*(4), 582–589. https://doi.org/10.1038/nn.3973

Wiseman, S., & Neisser, U. (1974). Perceptual Organization as a Determinant of Visual Recognition Memory. *The American Journal of Psychology*, *87*(4), 675–681. https://doi.org/10.2307/1421974

Wisse, L. E. M., Daugherty, A. M., Olsen, R. K., Berron, D., Carr, V. A., Stark, C. E. L., Amaral, R. S. C., Amunts, K., Augustinack, J. C., Bender, A. R., Bernstein, J. D., Boccardi, M., Bocchetta, M., Burggren, A., Chakravarty, M. M., Chupin, M., Ekstrom, A., de Flores, R., Insausti, R., … Group, for the H. S. (2017). A harmonized segmentation protocol for hippocampal and parahippocampal subregions: Why do we need one and what are the key goals? *Hippocampus*, *27*(1), 3–11. https://doi.org/10.1002/hipo.22671

Woolrich, M. W., Behrens, T. E. J., Beckmann, C. F., Jenkinson, M., & Smith, S. M. (2004). Multilevel linear modelling for FMRI group analysis using Bayesian inference. *NeuroImage*, *21*(4), 1732–1747. https://doi.org/10.1016/j.neuroimage.2003.12.023

Woolrich, M. W., Jbabdi, S., Patenaude, B., Chappell, M., Makni, S., Behrens, T., Beckmann, C., Jenkinson, M., & Smith, S. M. (2009). Bayesian analysis of neuroimaging data in FSL. *NeuroImage*, 45(1, Supplement 1), S173–S186. https://doi.org/10.1016/j.neuroimage.2008.10.055

Woolrich, M. W., Ripley, B. D., Brady, M., & Smith, S. M. (2001). Temporal Autocorrelation in Univariate Linear Modeling of FMRI Data. *NeuroImage*, 14(6), 1370–1386. https://doi.org/10.1006/nimg.2001.0931

Yassa, M. A., Mattfeld, A. T., Stark, S. M., & Stark, C. E. L. (2011). Age-related memory deficits linked to circuit-specific disruptions in the hippocampus. *Proceedings of the National Academy of Sciences*, 108(21), 8873–8878. https://doi.org/10.1073/pnas.1101567108

Yassa, M. A., & Stark, C. E. L. (2011). Pattern separation in the hippocampus. *Trends in Neurosciences*, 34(10), 515–525. https://doi.org/10.1016/j.tins.2011.06.006

Yonelinas, A. P. (2013). The hippocampus supports high-resolution binding in the service of perception, working memory and long-term memory. *Behavioural Brain Research*, 254, 34–44. https://doi.org/10.1016/j.bbr.2013.05.030

Yushkevich, P. A., Pluta, J. B., Wang, H., Xie, L., Ding, S.-L., Gertje, E. C., Mancuso, L., Kliot, D., Das, S. R., & Wolk, D. A. (2015). Automated volumetry and regional thickness analysis of hippocampal subfields and medial temporal cortical structures in mild cognitive impairment. *Human Brain Mapping*, 36(1), 258–287. https://doi.org/10.1002/hbm.22627